University of Texas at El Paso
DigitalCommons@UTEP

Open Access Theses & Dissertations

2019-01-01

A Study Of Solvent Effects On The Ground And Excited States Of Endohedral Tri-Scandium Nitride C80 Fullerene Coupled With Zinc Phthalocyanine And Metal-Free Phthalocyanine Using Dft-Pcm Method

Timilsina Prasad Timlsina
University of Texas at El Paso, sptimilsina@miners.utep.edu

Follow this and additional works at: https://digitalcommons.utep.edu/open_etd

 Part of the Condensed Matter Physics Commons, and the Oil, Gas, and Energy Commons

Recommended Citation
Timlsina, Timilsina Prasad, "A Study Of Solvent Effects On The Ground And Excited States Of Endohedral Tri-Scandium Nitride C80 Fullerene Coupled With Zinc Phthalocyanine And Metal-Free Phthalocyanine Using Dft-Pcm Method" (2019). *Open Access Theses & Dissertations*. 178.
https://digitalcommons.utep.edu/open_etd/178

This is brought to you for free and open access by DigitalCommons@UTEP. It has been accepted for inclusion in Open Access Theses & Dissertations by an authorized administrator of DigitalCommons@UTEP. For more information, please contact lweber@utep.edu.

A STUDY OF SOLVENT EFFECTS ON THE GROUND AND EXCITED STATES OF ENDOHEDRAL TRI-SCANDIUM NITRIDE C_{80} FULLERENE COUPLED WITH ZINC PHTHALOCYANINE AND METAL-FREE PHTHALOCYANINE USING DFT-PCM METHOD

SURYA PRASAD TIMILSINA

Master's Program in Physics

APPROVED:

Rajendra R. Zope, Ph.D., Chair

Tunna Baruah, Ph.D.

Ramon Ravelo, Ph.D.

Russell Chianelli, Ph.D.

Stephen Crites, Ph.D.
Dean of the Graduate School

Copyright ©

by

Surya Prasad Timilsina

2019

Dedication

To my Parents

A STUDY OF SOLVENT EFFECTS ON THE GROUND AND EXCITED STATES OF ENDOHEDRAL TRISCANDIUM NITRIDE C_{80} FULLERENE COUPLED WITH ZINC PHTHALOCYANINE AND METAL–FREE PHTHALOCYANINE USING DFT-PCM METHOD

by

SURYA PRASAD TIMILSINA, M.SC.

THESIS

Presented to the Faculty of the Graduate School of

The University of Texas at El Paso

in Partial Fulfillment

of the Requirements

for the Degree of

MASTER OF SCIENCE

Department of Physics

THE UNIVERSITY OF TEXAS AT EL PASO

May 2019

Acknowledgements

I would like to express my deepest appreciation to my committee chair, Dr. Rajendra R. Zope and Dr. Tunna Baruah, who provided valuable help through every step of my study and research, making my scientific background stronger. Without their great support and guidance this study would not have been possible.

I would also like to thank my committee members Dr. Ramon Ravelo and Dr. Russell Chianelli for providing me their valuable time and great help.

In addition, a sincere thanks to Dr. Luis Basurto, Dr. Yoh Yamamoto, and Dr. Jorge Vargas who helped me a lot in this work. I also thankful to my lab mates Parkash Mishra and Peter O Ufoundo for their valuable technical support.

Abstract

The photovoltaic active materials composed of endohedral metafullerene and phthalocyanine derivatives are known as excellent electron donor-acceptor pairs. The tri-metallic nitride endohedral C_{80} fullerene exhibits high absorption coefficients in the visible region of spectrum and have similar electron-accepting abilities as that of C_{60} fullerene, which can allow for higher efficiencies in OPV devices. In this study, we examine the effect of solvent on the charge transfer excitation energies of $Sc_3N@C_{80}$–ZnPc and $Sc_3N@C_{80}$–H_2Pc donor-acceptor molecular complexes. Three different solvents with different polarity - water, toluene, and acetone are used. The solvent is modeled as a polarizable continuum as implemented in our UTEP-NRLMOL code. The charge transfer excitation energy is proportional to the open circuit voltage which is a parameter that determines the efficiency of photovoltaic cell. We compute the charge transfer excitation energies using the perturbative delta-SCF method developed in our laboratory. The charge transfer excitation energies, in general, decreases in solutions with respect to its gas phase values. The stabilization of charge-transfer states increases with increase in the solvent polarity. A detailed orbital analysis of the ground and excited states is performed. We find that the presence of solvents can reorder the orbitals of the solute complexes as compared to gas-phase orbital order as well change the character of the excited states. The effect of the solvent on local excitations are small as compared to the charge transfer excitations. We find that there are few pure charge transfer states for $Sc_3N@C_{80}$–ZnPc unlike in $Sc_3N@C_{80}$–H_2Pc for each solvents taken.

Table of Contents

List of Tables

List of Figures

Chapter 1: Introduction

1.1 Objective

In near future fossil fuels, which are dominant sources of energy in present, are no longer available for us to fulfill the needs of energy. The growing needs of energy and continual decreasing of fossil fuel resources is a pressing challenge for us to ensure sufficient access to energy for all of us. The prime aim of the research conducted and presented here to contribute in the widespread efforts that are being made with the aim of finding promising alternative energy resources in order to relieve our currently intense dependency on fossil fuel reserves.

We need energy in our everyday life form cooking food to running vehicles. The role of energy in human everyday life is unquestionably great. It is manifestly clear that the rely on the non-renewable energy resources for energy is no longer conceivable mainly because their sources are limited and continuously decreasing. Further, non-renewable energy sources like nuclear power plants are hazardous over their consumption. In order to alleviate the dire situation of energy crisis as well as environmental pollution due to their use, alternative bio-friendly energy sources are to be promoted. The idea of utilizing solar energy seems to be more appealing due to its vast advantages such as being a free, clean and abundant reserve. So far, various types of substitutes have been introduced and put into practice. This study focuses the potential application of materials used in the active layer of organic photovoltaic cells.

1.2 Organic Photo Voltaic Cells

Organic photovoltaic cells (OPVs) have drawn a considerable amount of attention in scientific community due to their distinctive properties for the development of solar cells. Organic materials have low specific weight, excellent mechanical and chemical flexibility, almost unlimited variability and high optical absorption coefficients [1–3] These unique properties make OPVs as ideal solar cells. Furthermore, the manufacture cost is low for the fabrication of OPVs.

In 1977 it is found that conductivity of carbon-based molecular and polymeric materials increased significantly by means of chemical doping [4]. Until that time, those materials were regarded as electrical insulators. In general, the conductivity of a p-type semiconductor can be boosted by adding n-type materials and vice versa. The electronic properties these semiconductors are related to the conjugation of carbon atoms, which means having alternate single and double bonds. In these materials, the gap between highest occupied molecular orbitals (HOMO) and lowest unoccupied molecular orbital(LUMO) varies from 1eV to 4eV which makes them perfect choice for utilization in optoelectronic devices in the visible range [5].

1.2.1 Bulk Heterojunction Organic Solar Cell

There are basically two types of organic solar cells, planer heterojunction and bulk heterojunction types. Diagram of the layered structure of a bulk heterojunction organic solar cell is shown below.

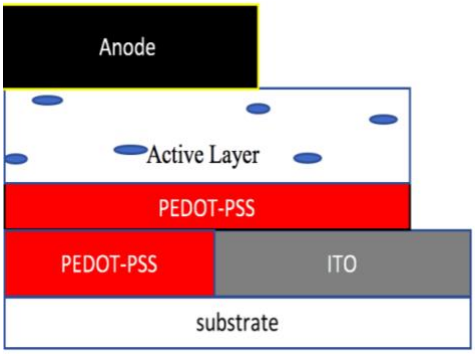

Figure 1.1: layered structure of a bulk heterojunction organic solar cell.

The organic solar cells consist of at least five distinct layers with substrate. The substrate can be glass or any transparent flexible material. A cathodic material, indium tin oxide (ITO), is placed on top of the substrate. A substrate coated with ITO is easily available and ITO is used as cathodic material because of its transparency. On the top of this cathodic material, a layer of the conductive polymer mixture poly (3,4-ethylenedioxythiophene)/poly (styrenesulfonate) (PEDOT–

PSS) [6] is placed which serves as a hole carrier and exciton blocker. Beside this, PEDOT–PSS layer also smoothens out ITO surface and prevents active layer from oxygen, which can damage the active layer. There is an active layer on top of the PEDOT–PSS, which is responsible for light absorption, exciton generation and dissociation as well as charge carrier diffusion. The topmost layer is the anode.

1.2.2 Power Conversion Efficiency Factors

The power conversion efficiency of OPVs depends upon open circuit voltage V_{oc}, short circuited current I_{sc}, power density of incident radiation (P_{in}) and fill factor (F_f) as:

$$\eta = \frac{V_{oc} I_{sc} F_f}{P_{in}} \tag{1.1}$$

Brabec et al. described the linear relation between the LUMO level of the fullerene acceptors and V_{oc} [7] and Scharber et al. conveyed the linear correlation between HOMO level of the donors and the V_{oc} [8]. Therefore, V_{oc} is a sensitive parameter of the donor-acceptor's energy levels. This implies that in OPVs, V_{oc} is linearly proportional to the HOMO of the donor and LUMO of the acceptor. It becomes an active area of research to identify the proper donor-acceptor pairs that provide large open circuit voltage V_{oc} for efficient OPVs. Therefore, the present study focuses merely on increasing the open circuit voltage. The other factors that affect efficiency of OPVs are describe shortly below.

The short circuit current (I_{sc}) is directly related to the photo induced charge carrier density and charge carrier mobility in the organic semiconductor. It is a device parameter which is sensitive to the nano-morphology of active layer [8] OPVs which in turn depends on the film preparation details. The ratio of the actual maximum power available to the product of the open circuit voltage and short circuit current gives the fill factor. It is tied to the number of charge carriers reaching

the electrodes. Basically, the charge carrier recombination and transport are two hostile events and to achieve a high fill factor, the product of the lifetime of the charge carriers and their mobilities, which determines the distance that they can travel in a given electric field, has to be maximized [7]

The mechanism of the photo-induced charge transfer process that takes place in a donor-acceptor based organic photovoltaic device starts with production of excitons. When a photon of sufficient energy strikes the layer of D/A blend, the donor molecule of it absorbs energy form light and makes electron transfer from its HOMO to the LUMO of acceptor thereby creating a particle-hole pair called exciton. The figure below illustrates how exciton dissociation produces free charge carrier at the heterojunction.

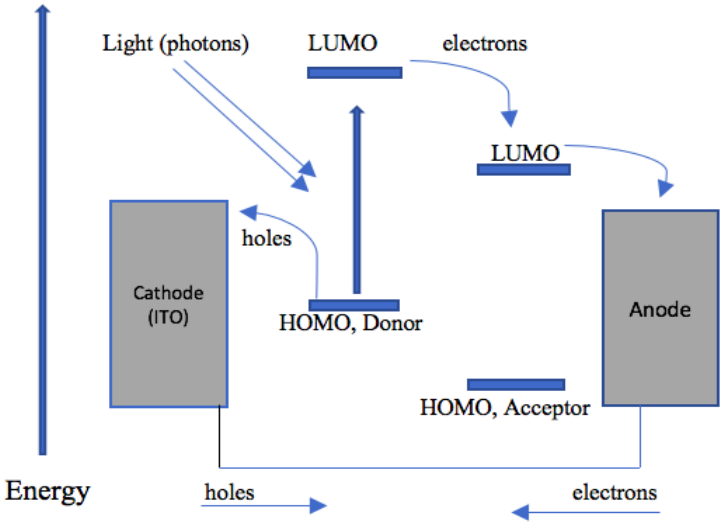

Figure 1.2: Schematic diagram of the band structure of heterojunction organic solar cell

The excitons are quasiparticles and bounded by coulomb forces .The excitons produce new states within the forbidden band gap and are detectable through optical transitions with known energies [7]. Based on the spin of the electrons and holes, excitons are classified into two types, they are singlet and triplet excitons. If both of the electron and the hole have the same spins, it is

called a triplet exciton and if the electron and the hole have opposite spins, then it is named a singlet exciton. The singlet and triplet excitons can be understand by means of diagram as:

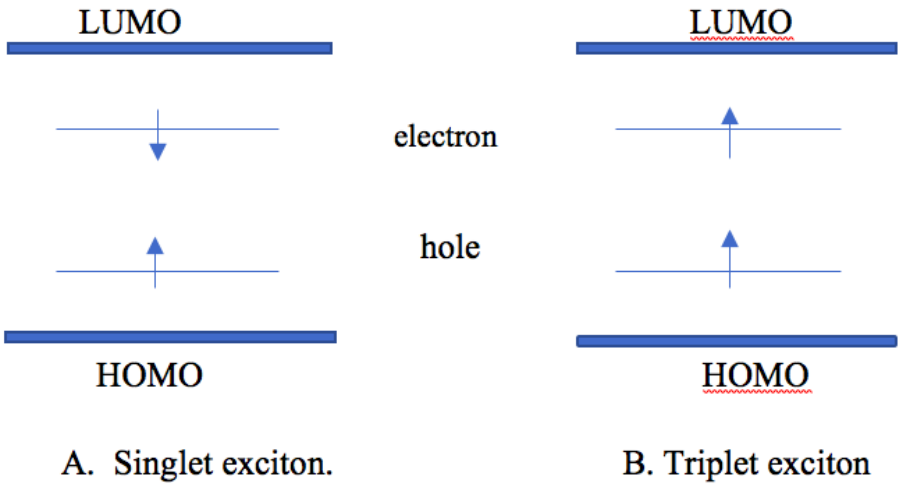

Figure 1.3: Schematic diagram of singlet and triplet excitons

During photo-excitations, free charge carriers are produce in D/A blend in the ratio of 1:10 in comparison to photo excitons due to exciton dissociation [8]. The exciton dissociation occurs efficiently in strong electric fields which can be applied either externally or through D/A interfaces due to their different work functions. Thus, the exciton origination occurs in the close vicinity to the donor-acceptor interface, within the exciton diffusion length. The exciton diffusion length is the average distance that an exciton can diffuse through a material before its annihilation due to recombination. The generated excitons can also decay without any contribution to the electrical current. This means that thickness of active layer of OPVs affects significantly for open circuit voltage. Bulk heterojunction cell can be made more efficient by mixing the donor and acceptor, which increases the interfacial area and reduces the distance that excitons need to travel to reach the interface [5] .

Next, created free charge carriers are to be collected using appropriate electrode [6] before they die by recombination. For this, the desired driving force is delivered by the gradient in the chemical potentials of electrons and holes (quasi Fermi levels of the doped phases) created in the donor-acceptor junction. This gradient is determined by the difference between the HOMO level

of the donor (quasi Fermi level of the holes) and LUMO level of the acceptor (quasi Fermi level of the electrons). This internal electric field, which is the negative gradient of chemical potential, functions in drifting charge carriers and determines the maximum open circuit voltage of OPVs. It is important to point out that at each intervening step, the process may settle back to the ground state by utilizing energy either in the form of heat or electromagnetic radiation [2]. The electrons and holes are transported in suitable cathode and anode respectively.

The charge separation takes place in the following steps as shown. In the diagram, D and A respectively represent donor and acceptor while δ pictures the fraction of the charge transfer which ranges from 0 to 1. It is 0 if there is no charge transfer and if it is 1 then whole charge (electron) gets transferred [2].

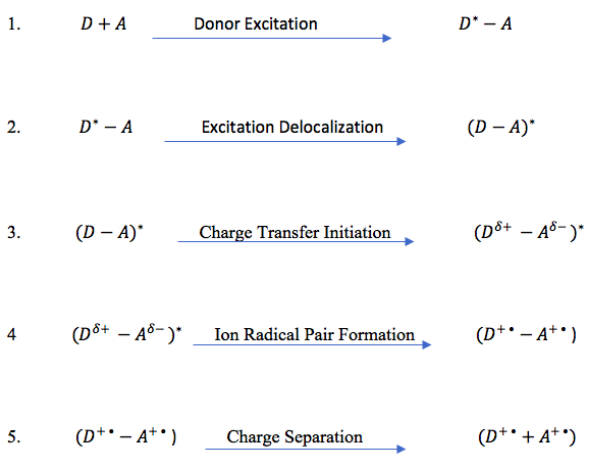

Figure 1.4: Mechanism of charge separation in donor-acceptor pairs

A characteristic feature of the charge transfer process in D-A theories is that the orbitals that take place in the electron transfer are well separated spatially with vanishing overlap [9].

In principle, only a small part of the incident solar radiation is collected by organic materials due to their large band gap. Therefore, materials having small band gaps are desired to utilize as the donor molecule [3,8]. In addition, in order to increase the probability of photon

absorption by the device, some antenna systems can be added to the donors which can expand wavelength range of incident photons to cause excitation. Unlike other materials, chromophores with antenna possess high absorption coefficients in a certain range of wavelengths and therefore a wide range of wavelengths will be covered by the donor molecule. There should be a fast energy transfer among the chromophores in order to compete with the excited states' relaxation by other processes like fluorescence. Two factors that affect the energy transfer are the distance between any two chromophores and their relative orientation. Antenna systems also add control and photo protective mechanisms to the system, as in natural photosynthesis. Evidently, a higher photon absorption rate can be directly proportional to a higher efficiency for the cell [10].

1.3 MATERIALS USED FOR THIS STUDY

In hetero junction solar cell, the active layer is made by a donor and an acceptor. Fullerene and its derivative are common acceptors for OPVs while Poly-(phenylene vinylene) derivatives and poly-(alkyl-thiophenes) [6] are commonly used as donors. Besides, other chomophores such as phthalocyanine derivatives can also be employed as donors. In the current study two phthalocyanines derivatives viz. $Sc_3N@C_{80}$–ZnPc and $Sc_3N@C_{80}$–H_2Pc as donor-acceptor blend are studied for the potential application in OPVs in different solvents. The aim of this study is to achieve improved power conversion efficiency of OPVs using these materials as active layer components in solutions.

As mention earlier, the present study focuses the solvents effect on charge transfer properties of endohedral tri-scandium nitride C_{80} (I_h) fullerene coupled with zinc phthalocyanine and zinc-free phthalocyanine. A gas phase study was carried out by Basurto et al. earlier which showed that a rather larger charge transfer energy can be achieved using these materials. This study also pointed out that orientation of endohedral unit in C_{80} cage does not influence charge transfer significantly [11], while Amerikheirabadi et al. mentioned that among phalocynanine

families, fullerene and phthalocyanine with a metal center are more favorable candidate of D-A pair [12].The charge transfer from the donor to the acceptor molecule creates a large dipole on the pair which can induce dipoles on the surrounding. To simulate this effect we consider the surrounding effect as solvent. The interaction between the solute dipole and the induced dipole on the solvent leads to stabilization of the excited state energies. To explore solvent effect on charge transport properties, this research is carrying out by taking the same D-A complexes as taken in the gas phase study by Amerikheirabadi et al. [12]. The molecular details and properties of the individual components of electron-donor-acceptor molecular complexes are given in the following sub-section.

1.3.1 Isolated Components

We are taking a pair of electron-donor complexes viz. $Sc_3N@C_{80}$–H_2Pc and $Sc_3N@C_{80}$–ZnPc. $Sc_3N@C_{80}$–H_2Pc is composed of $Sc_3N@C_{80}$ and H_2Pc where as $Sc_3N@C_{80}$–ZnPc formed by coupling between $Sc_3N@C_{80}$ and ZnPc. In this sub-section, brief information of the individual components of these complexes are presented here.

Let us start with phthalocyanine (H_2Pc) which is a large macrocyclic, two-dimensional aromatic organic compound with four isoindole units linked by nitrogen atoms. There are 18 π electrons which can be delocalized extensively thereby affording the molecule useful characteristics. The molecular structure is shown in the figure below.

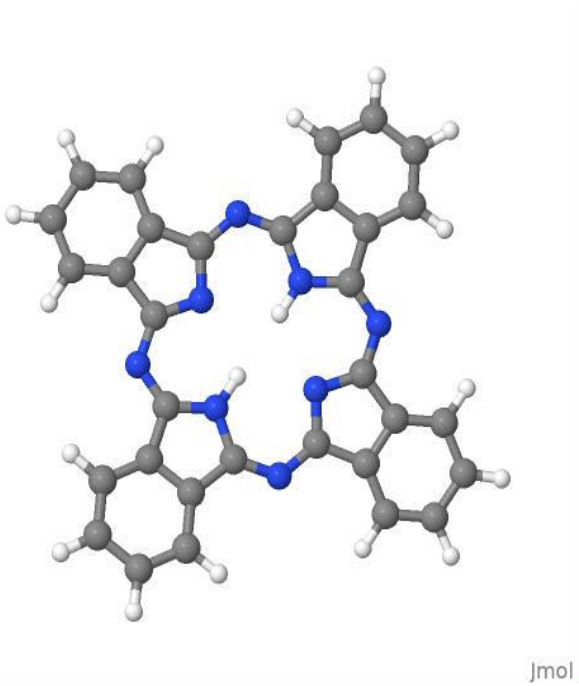

Figure 1.5: Optimized structure of pthalocyanine (H_2Pc) molecule

A phthalocyanine (H_2Pc) molecule has molecular formula $(C_8H_4N_2)_4H_2$), which has 58 atoms. Among them 8 are nitrogen atoms which are indicated by blue color in the figure, 18 hydrogen atoms (white) and remaining 32 are carbon atoms with 266 electrons. The inner ring of H_2Pc contains 8 Carbon atoms and 8 Nitrogen atoms alternatingly with varying bond lengths form 0.132 nm to 0.139nm.

Zinc Phthalocyanine is another isolated complex used in this study .The molecular formula of ZnPc is $(C_8H_4N_2)_4Zn$) which has 57 atoms and 294 electrons. Zinc phthalocyanine is derived by combining the conjugate base of H_2Pc i.e. Pc^{--} with Zinc. The molecular structure is shown in figure below.

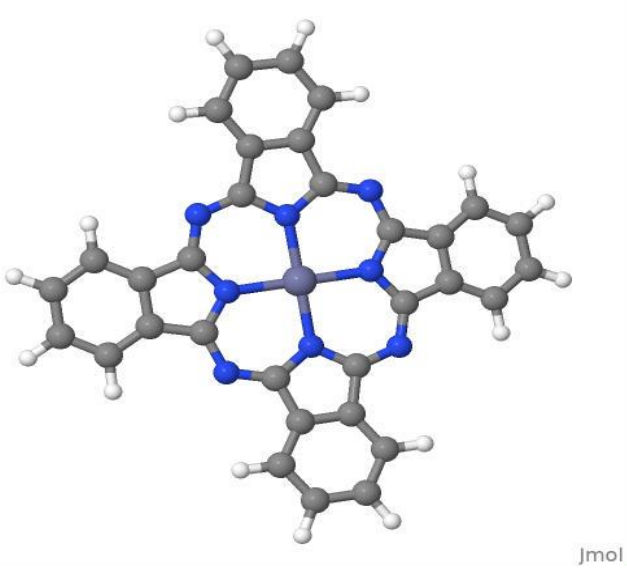

Figure 1.6: Optimized structure of Zinc pthalocyanine (ZnPc) molecule

In ZnPc, Zn lies at the center of the ring of 16 alternate nitrogen and hydrogen atoms such that only N atoms are bonded with Zn. The ring is slightly curved with central at Zn atom as three of angles between two nitrogen and Zinc are 89.9° and the next is 90.2°. The bond length of alternate Carbon and nitrogen bonds vary from 0.133nm to 0.138 nm while the three N and Zn bonds are 0.2 nm long and the remaining is 0.199 nm long.

Next, endohedral tri-scandium nitride C–80 fullerene is used in the present study. The structure of $Sc_3N@C_{80}$ is shown in the figure below.

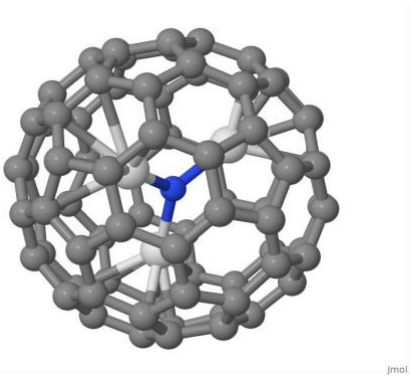

Figure 1.7: Optimized structure of a $Sc_3N@C_{80}$ molecule obtained through Jmol viewer

The structure of $Sc_3N@C_{80}$ is symmetric which is verified by Raman and infrared spectroscopy study [13]. In $Sc_3N@C_{80}$, Sc_3N is entrapped in the cage of C_{80} fullerene. The bond lengths between Scandium and Nitrogen in Sc_3N are 2.04 Å and the average 6:6 and 5:6 bond lengths in $Sc_3N@C_{80}$ are 1.43 Å and 1.45 Å respectively. After C_{60} and $C_{70,}$ $Sc_3N@C_{80}$ is the most abundant fullerene which can be produced under ordinary conditions. A stable molecule is formed by combining C_{80} cage, which is symmetric spherically, and the endohedral unit Sc_3N [14]. There is evidence that the Sc_3N moves freely inside the fullerene cage [15]. $_{21}Sc^{45}$ is the most commonly used metal in the formation of tri-metallic nitride endohedral fullerenes. The encapsulation of Sc_3N body in C_{80} possesses a strongly exothermic mechanism [16]. As there are 80 vertices and 120 edges in C–80 carbon cage, C_{80} fullerene is composed of 12 pentagons and 30 hexagons. It has been identified that there are two stable isomers of $Sc_3N@C_{80}$, one in which C_{80} possesses icosahedral (I_h) symmetry while in the next C_{80} cage exhibits a D_{5h} symmetry. The structures which possess I_h symmetry are more abundant. The endohedral unit (Sc_3N) displays a trigonal planar geometry for both of these symmetric isomers [17]. In $Sc_3N@C_{80}$ (I_h), there are pyrene, 6:6 bond abutted by a hexagon and a pentagon, and corannulene, 6:5 bond abutted by two hexagons, sites while reactive pyracylene sites, a 6-6 bond abutted by two pentagons [18] are missing which suppose $Sc_3N@C_{80}$ possesses unique chemical behavior. Both the (symmetric) isomers of $Sc_3N@C_{80}$ have optical band gap greater than 1eV, so are considered as large band gap fullerenes [17].

The study of the electronic properties of $Sc_3N@C_{80}$ revealed that the endohedral unit Sc_3N gives unto six electrons to the outer fullerene cage. The mechanism of transfer of electrons occurs as $[Sc_3N]^{+6}@[C_{80}]^{-6}$ [17] causing a closed shell configuration for the endohedral fullerene. Due to low-lying unoccupied orbitals [15], fullerenes, generally, exhibit large electron affinities, high charge accumulation and, low reorganization energies in the charge transfer reactions. Due to these properties, fullerenes serve as ideal candidates as acceptors in D-A complexes [19,20].Therefore, as other fullerenes, $Sc_3N@C_{80}$ possesses small reorganization energies during charge transfer

reactions [21].This can be utilized as an acceptor component in organic photovoltaic (OVPs) solar cells to increase the lifetime in the order of few nano- seconds of the charge separated state [21].

1.3.2 Electron-Donor-Acceptor Complexes

In this study the complexes formed by a weak coupling of endohedral tri-scandium nitride C–80 fullerene with zinc phthalocyanine (ZnPc) and phthalocyanine (H_2Pc) compounds are investigated. The molecular structures and their characteristics are explained in brief here.

The molecule $Sc_3N@C_{80}$_ZnPc is comprised of 141 atoms and 844 electrons. The molecular structure of this complex obtained by placing two components ZnPc and $Sc_3N@C_{80}$ co-facially is as shown in figure below.

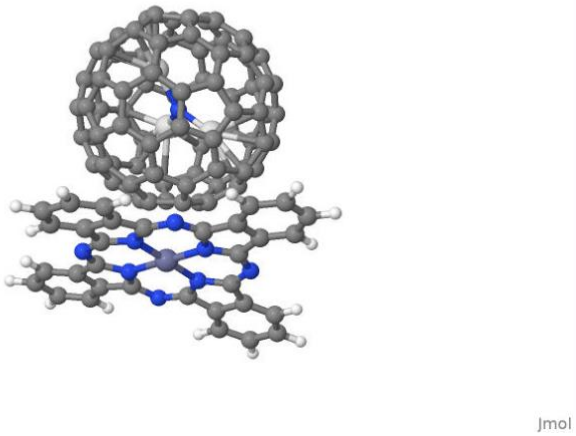

Figure 1.8: Optimized structure of $Sc_3N@C_{80}$–ZnPc

The distance between the nearest carbon atom of $Sc_3N@C_{80}$ to Zn atom of ZnPc plane is 0.317 nm, which is the smallest donor-acceptor surface-to-surface distance. The binding of this complex is due to the van der Waals force. The binding energy of the system calculated using DFT in PBE functional by supramolecular approach is 0.2964 eV and the dipole moment is found to be 0.32 D.

The complex $Sc_3N@C_{80}$_H_2Pc is comprised of 142 atoms and 816 electrons. The molecular structure of this complex obtained by placing two components H_2Pc and $Sc_3N@C_{80}$ co-facially is as shown in figure below.

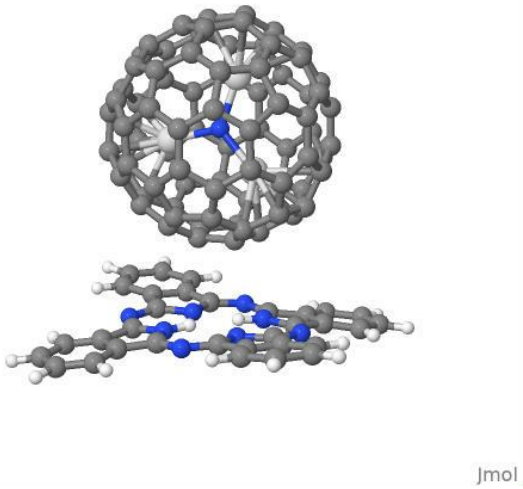

Figure 1.9: Optimized structure of $Sc_3N@C_{80}$_H_2Pc

As in $Sc_3N@C_{80}$–ZnPc, the binding is due to the weak van der Waals force and the binding energy is calculated using supramolecular approach in DFT level using PBE functional is 0.22 eV and total dipole moment is 1.4 D. The smallest surface-to-surface distance in this donor-acceptor pair is 0.316 nm which is little less than surface-to-surface distance of $Sc_3N@C_{80}$–ZnPc.

1.3.3 Donor-Acceptor Orientation

One of the factors influencing the charge transfer energetics of the complexes is the relative orientations of the donor and acceptor components which can be placed either in a co- facial or an end-on configuration. These variations create different associated local electric fields which make a shift in HOMO and LUMO energy levels influencing the exciton dissociation at the D-A interface. The surface-to-surface interaction of the D-A is largest in co-facial alignment . The polarization effects arising from the interaction of the D-A charge distributions, which change the energy levels, are decreased in going from co-facial to end-on orientation [20]. Likewise, the

strength of the non-covalent $\pi - \pi$ interactions is decreased in end-on geometry compared to those in co-facial alignment. As a result, the CT excitation energies are larger for the end-on geometry than the co-facial structure due to a lower exciton binding energy in end-on orientation [20]. Practically, in the active layer of OPV cells a combination of different orientations may co-exist [20]. However, all the dyads studied in this work are in co-facial position. Another influential element in the CT energies is the distance between the donor and acceptor parts; however, its effect is less than the relative D/A pair orientations [20].

1.4 REASONS OF CHOOSING THESE MOLECULES

Metal containing endohedral fullerenes and phthalocyanine derivatives are known as excellent candidates for the active materials in the OPVs. The tri-metallic nitride endohedral C_{80} fullerene have the maximum absorption coefficients in the visible region of spectrum and have electron accepting abilities similar to C_{60} fullerene which can allow for superior efficacies in OPV devices. Besides, the endohedral metafullerens (EMFs) have small reorganization energies and have capacity to fine-tune their HOMO–LUMO gaps with different embedded unit inside make them suitable candidates as electron acceptors. EMFs of type $M_3N@C_{80}$ with M= Sc, Y, Gd, Tb, Dy, Ho, Er, Tm, Lu acquire a reduced LUMO offset of donor/acceptor there by offer the possibility of significant increase in the power conservation efficiency. The electron donor-acceptor molecular complex $Sc_3N@C_{80}$–ZnPc is taken for study mainly because the Zinc phthalocyanine is the best performing donor molecule and $Sc_3N@C_{80}$ is excellent acceptor. Besides, $Sc_3N@C_{80}$–ZnPc had been studied in vacuum earlier in our lab and established this molecular complex as a better candidate as active material to be used in OPVs than $Sc_3N@C_{80}$–H_2Pc. Therefore, solvent effect of $Sc_3N@C_{80}$–ZnPc in variant polarity is studying here and $Sc_3N@C_{80}$–H_2Pc is taken for comparison of the results with metal containing $Sc_3N@C_{80}$–ZnPc complex.

1.3 SOME DEFINITIONS

Experimental evidence states that the open circuit voltage, V_{oc}, of OPVs which is one of the determining factors in power conversion efficiency (PCE) of these devices, is directly related to the photo-induced charge-transfer (CT) excited state energies [9]. It has been found that CT excitation energies depend completely on the ground-state properties of the separated systems [22]. The lowest CT excitation energies can be approximately calculated using the following formula known as Mullikan's equation;

$$E_{ex} = IP^D - EA^A - \frac{1}{R} \tag{1.2}$$

where IP^D and EA^A denote the ionization potential of the donor and electron affinity of the acceptor respectively and R gives the hole-electron separation [23,24]. The 1/R term is the coulomb energy originating from the electrostatic interaction between the charged donor and acceptor species. It is commonly calculated using partial charges on donor-acceptors in the coulomb energy expression [20].

The ionization potential (IP^D) of a neutral molecule (with N electrons) is given by the following expression;

$$IP^D = E(N-1) - E(N) \tag{1.3}$$

where $E(N)$ is the total energy of the molecule in its ground state and $E(N-1)$ is the total energy of the optimized cation. Likewise, the electron affinity (EA^A) of a neutral molecule (with N electrons) is calculated by the following expression;

$$EA^A = E(N) - E(N+1) \tag{1.4}$$

where E(N+1) is the total energy of the optimized anion. These are usually called adiabatic IPs and EAs. However, if the structures of the cations and anions are not relaxed (optimized), the calculated energy difference between the optimized neutral structure and ions at the geometry of neutreal are called vertical IPs and EAs . The quasi-particle gap of charge transfer complex is estimated by subtracting vertical electron affinity form the vertical ionization paternal. Another important term we study here is the optical gap which is given by HOMO-LUMO excitation energy.

Using perturbative delta-SCF method [20,22], triplet and mixed states energy are obtained whereas singlet state energy is estimated using Ziegler-Rauk Method [25]. If E_M and E_T are mixed state and triplet state for a particular transition then singlet excited state energy (E_s) is calculated by using the mentioned method as:

$$E_S = 2E_M - E_T \tag{1.5}$$

Triplet state is a state where total spin is equal to 1 or spin multiplicity is equal to 3 and for singlet state to total spin is 0 and spin multiplicity is 1. The mixed state energy is average of singlet and triplet states i.e. a 50-50 blend of pure singlet and triplet states.

Chapter 2: Theoretical Background and Computational Methods

2.1 INTRODUCTION

The wave-function of a physical system is a fundamental quantity which gives nearly a complete picture of the system form subatomic to atomic to macroscopic level. The wave-function is a solution o

$$i\,\hbar\frac{\partial}{\partial t}\psi(\boldsymbol{r}\,,t)=\hat{H}\psi \tag{2.1}$$

This is a partial differential equation called time dependent Schrodinger equation (SE) which illustrates how quantum state of a system evolves with time. In equation (2.1), $\psi\ and\ H$ represent wave function and Hamiltonian of the system. Generally, $\Psi\ (\boldsymbol{r},t)$ is a many-body function containing coordinates for all the degrees of freedom in a system, as well as time.

The physical properties of most of the simple systems depends upon the ground state wave function. The consideration of the SE enables us to determine the electronic ground state of the system. By minimizing the total energy with respect to all the degree of freedom in wave function, the ground state wavefunction of the system can be found. To solve SE, the Hamiltonian of system is known.

The complete many-body Hamiltonian [26] for a system of interacting electrons and nuclei is given by

$$\hat{H}=\ -\frac{\hbar^2}{2m_e}\sum_i\nabla_i^2\ \ -\frac{\hbar^2}{2M_I}\sum_I\nabla_I^2-\sum_{i,I}\frac{z_Ie^2}{|\boldsymbol{r_i}-\boldsymbol{R_I}|}+\frac{1}{2}\sum_{i\neq j}\frac{e^2}{|\boldsymbol{r_i}-\boldsymbol{r_j}|}\ +\frac{1}{2}\sum_{I\neq J}\frac{z_Iz_Je^2}{|\boldsymbol{R_I}-\boldsymbol{R_J}|} \tag{2.2}$$

The lower case subscripts represent electronic quantities while the upper case represent the nuclear quantities. Electrons have a mass m_e and charge e, nuclei have mass M_I and charge Z_I, $\boldsymbol{R_I}$ and $\boldsymbol{r_i}$ are the positions of the nuclei and electrons respectively.

The equation (2.2) includes coulombic interactions between the electrons and between the electrons and the nuclei in the Hamiltonian which can be also be written as;

$$\hat{H} = \hat{T}_e + \hat{T}_n + \hat{V}_{ext} + \hat{V}_{int} + \hat{V}_{n-n} \tag{2.3}$$

where $\hat{T}_e$ and $\hat{T}_n$ are the kinetic energy operators of the electrons and ions respectively. The potential of nuclei are viewed as 'external' [26] from the electronic point of view and potential of electrons are 'internal' [26]. Therefore the notations $\hat{V}_{ext}$ and $\hat{V}_{int}$ represent the coulombic potential energy of nuclei and electrons, and electrons with themselves respectively. The fifth term of equation (2.3) i.e. $\hat{V}_{n-n}$, accounts the coulombic interaction of the nuclei with one another.

For the hydrogen like systems, the Schrödinger equation with this Hamiltonian can be solved with reasonable accuracy. However, the analytical solution of Schrodinger equation for most systems, it is practically impossible to solve with precision with the given Hamiltonian. Thus, to transform complex many-body Schrödinger equation into a simple tractable problem, a few approximations are proposed, which are explain concisely in the forthcoming sections.

2.2 BORN-OPPENHEIMER APPROXIMATION

In the many body Hamiltonian of equation (2.2), due to great difference in masses of nucleus and electrons i.e. $M_I \gg m_e$ there is asymmetry in $\hat{T}_e$ and $\hat{T}_n$. Due to this fact, we can break the complex problem representing by the equation (2.4) into two simpler ones viz. electronic and nuclear parts [27] . The breaking of total wave-function of a system into its electronic and nuclear parts is explained in terms of Born-Oppenheimer (BO) approximation [28]. Thus in BO approximation:

$$\psi_{total} = \psi_{elec} \times \psi_{nuc} \tag{2.4}$$

Since $M_I \gg m_e$,we can consider that nuclear motion is negligibly small and we can evaluate electronic part, ψ_{elec}, of the wave function by considering electrons interact within a fixed nuclear potential. Therefore, electronic Schrödinger wave equation can be written as:

$$\hat{H}_e(\boldsymbol{r}, \boldsymbol{R})\psi_{elec}(\boldsymbol{r}, \boldsymbol{R}) = E_e\psi_{elec}(\boldsymbol{r}, \boldsymbol{R}) \tag{2.5}$$

In equation (2.5), $\boldsymbol{r}$ and $\boldsymbol{R}$ represent the electronic coordinates and the coordinates of the nuclei respectively. Here, $\hat{H}_e$ is the electronic Hamiltonian in which nuclear kinetic energy term, $\hat{T}_n$, and the nuclear-nuclear interaction ($\hat{V}_{n-n}$) terms are excluded. The electrons interact with the nuclei through their respective coulombic potential energy terms. The electronic energy eigenvalues E_e are dependent on the nuclear positions ($\boldsymbol{R}$). The potential for the Schrodinger equation containing only the nuclei is generated by solving ψ_{elec} as;

$$\hat{T}_n + E_e(\boldsymbol{R})]\psi_{nuc}(\boldsymbol{R}) = E\psi_{nuc}(\boldsymbol{R}) \tag{2.6}$$

where E is the energy eigenvalues for the entire system. In several cases, nuclear kinetic energy term ($\hat{T}_n$) and interaction potential term ($\hat{V}_{n-n}$), are solved classically and supplemented to the electronic result.

The BO approximation generally gives an excellent estimation for most purposes.

2.3 DENSITY FUNCTIONAL THEORY

Generally, the solution of many-body Schrödinger Equation with Hamiltonian given in Eq.(2.2) is difficult to get even with the use of BO approximation. The Density Functional Theory (DFT) is an approach which transforms a complex many-particles interacting problem into an independent particles problem acting within an effective potential. The effective potential is characterized as mean-field resulting from the other particles in the system [26].

Density Functional Theory (DFT) is a theory of interrelated many-body systems, which is a principal tool for the condensed matter electronic structure calculation as well as for the quantitative studies of molecules and other finite systems. The basic idea of DFT is that any properties of many particles system can be observed as a functional of the ground state density $n_0(\boldsymbol{r})$ instead of wave functions. We can determine the entire information in the many-body wave functions for the ground state and excited states if ground state density of the system is known. That means knowing the ground state density is equivalent to knowing the wave function for the ground state and all excited states as well. The word 'functional' refers 'function of a function'. Within Khon-Sham formalism, the Hamiltonian of Eq.(2.4) operating on a 3N-dimensional wave can be replaced by independent-particle wavefunction and can derive all the essential features of a given system from the ground state density in three dimension [27].

The BO approximation allows us to treat the electrons distinctly from the nuclei. The nuclei are generally omitted as an external potential V_{ext} in which the electrons rest into their ground state. The kinetic energy due to nuclei and nuclear-nuclear potentials energy are often treated separately as in classical calculation. Thus, for the electrons, the Hamiltonian of Eq.(2.2) bears the form;

$$\widehat{H} = -\frac{\hbar^2}{2m_e}\sum_i \nabla_i^2 + \frac{1}{2}\sum_{i\neq j}\frac{e^2}{|\boldsymbol{r_i}-\boldsymbol{r_j}|} + \sum_i V_{ext}(\boldsymbol{r_i}) \tag{2.7}$$

Due to the electrons self-interaction term, the complex many-body problem represented by equation (2.9) cannot be reduced into further simpler single-body equation form. The Hohenberg-Kohn theorems stipulate the way of solving equation (2.9) by allocating a unique significance to the ground state density of particle [29].

2.3.1 Hohenberg-Kohn Theorems

There are two theorems put forward by Hohenberg and Kohn on which DFT is based. They are given as following:

Theorem **I** : For any number of particles are acting in an external potential ($V_{ext}(\boldsymbol{r})$) , then ground state energy is uniquely determined by the ground state density of particles ($n_0(\boldsymbol{r})$).

A consequence to the theorem **I** is that since the Hamiltonian is uniquely determined, except for a constant change in energy. Thus all the properties of the system can be derived completely knowing the ground state density [26].

Theorem II : For any $V_{ext}(\boldsymbol{r})$ we can define a universal functional for the energy $E[n]$ in terms of particle density $n(\boldsymbol{r})$. The density that minimizes this energy functional is the true ground state density $n_0(\boldsymbol{r})$.

The proof of theorem **II** based on the consequence of theorem **I**, which is, all the characteristics of a system can uniquely determine by the particle density $n(\boldsymbol{r})$. Every property including total energy can be expressed as a functional of particle density and we can rewrite Eq (2.3) as:

$$E[n] = T_e[n] + E_{int}[n] + \int d^3r\, V_{ext}(\boldsymbol{r})\, n(\boldsymbol{r})$$
$$= F_{HK}[n] + \int d^3r\, V_{ext}(\boldsymbol{r})\, n(\boldsymbol{r}) \tag{2.8}$$

Where, $E[n]$ is the energy functional in Hohenberg-Khon approach. The density-dependent functional $F_{HK}[n]$ called universal functional which includes the kinetic $T_e[n]$ and potential energy E_{int} (and, the energy terms neglected above for simplification) of the interacting electrons.

The energy functional $E[n]$ always gives the minimum energy for the ground state density. Moreover, if the functional $F_{HK}[n]$ is known, the minimization of the total energy of the system allows us to modify the particle density. Thus, to figure out the exact ground state density and

energy, known value of $E[n]$ is sufficient. One of the main difficulty here is that the functional $F_{HK}[n]$ depends on many-body correlations which is normally indefinite for everything except the simplest systems.

Theoretically, from the ground state density we can obtain all the information of the given system. Nevertheless, usually the relations from density to physical properties tend to be very indirect even for simple systems. For example, take a case of non-interacting electrons in an external potential; even though the exact functional $F_{HK}[n]$ is basically the kinetic energy, there is no straightforward way to get the kinetic energy starting from the density of the system. To obtain it, we have to determine the set of wave- functions of N multi-body system and start from there. The DFT had further refined by Kohn and Sham that permits us to make calculations to the real ground state functional.

2.3.2 Kohn-Sham Equations

The reformulation of the complex many-body Hamiltonian given in Eq.(2.2) as an independent particle system that yields precisely the same ground state density was made by Kohn and Sham to make DFT feasible. In principle, the electrons are presumed to be unrelated except for what is required to fulfil the exclusion principle. An effective potential is then combined to approximate the effects of many-body correlation without having explicit interaction term in the Hamiltonian. With these change, the problem becomes density dependent rather than the wave functions.

Evidently, we can show the density of lowest lying state of the complex many-body interacting system can be produced from a simpler independent system of particles. All the multi-body interactions are dumped into an effective potential in which the electrons move. What we have left are a set of independent particle equations which can be solved exactly:

$$\left(-\frac{\hbar^2}{2m}\nabla^2 + V_{eff}(\boldsymbol{r_i})\right)\varphi_i = \epsilon_i\varphi_i$$

(2.9)

where φ_i are the independent particle orbitals, ϵ_i is energy Eigen value and $V_{eff}(\boldsymbol{r})$ is the effective potential. In a system of N electrons, there are exactly N lowest energy orbitals for the ground state. The density of such system is obtained by summing over the densities of each orbitals as;

$$n(\boldsymbol{r}) = \sum_{i}^{N} |\varphi_i(\boldsymbol{r})|^2$$

(2.10)

And effective potential is given by:

$$V_{eff}(\boldsymbol{r}) = V_{ext}(\boldsymbol{r}) + \int \frac{n(\boldsymbol{r'})}{|\boldsymbol{r} - \boldsymbol{r'}|}\, d\boldsymbol{r'} + \frac{\delta E_{xc}[\boldsymbol{r}]}{\delta n(\boldsymbol{r})}$$

(2.11)

The 2nd and 3rd terms in (2.11) represent the electron-electron and the exchange-correlation interactions.

To solve the KS equations, the independent particle SE needs to be solved under consistent effective potential $V_{eff}(\boldsymbol{r})$ and density $n(\boldsymbol{r})$. Self-consistency is achieve by changing $V_{eff}(\boldsymbol{r})$ and $n(\boldsymbol{r})$ successively while solving. In the first step, an initial electron density is guessed. By considering the variation of the total energy functional with respect to electron density, the effective potential is then calculated.

The Eq.(2.9) can be solved with this effective potential as an eigenvalue problem. Optimization of this step demands most of the computational effort in solving the eigenvalue problem. Ultimately, we can evaluate the new particle density and convergence is tested. The new

density is generally some average of the old and new densities because of stability issues. The eigenvalue problem has a solution, once achieving self-consistency, if not then V_{eff} is calculated again and again for the new density until we have self-consistency.

2.4 EXCHANGE AND CORRELATION FUNCTIONAL

Although the DFT is exact theory, it needs the use of approximations, mainly because of the two reasons. The first one is BO approximation and next is due to some unknown exact form of the functional like exchange-correlation energy functional. Therefore, there exist different approximations like local density approximation, generalized gradient approximations, hybrid approximations, which help to approximate the functional within the Kohn-Sham formulation. We use the Generalized Gradient Approximation (GGA) in DFT calculations in NRLMOL code, which is explained briefly followed by Local Density Approximation (LDA) in the following subsections.

2.4.1 Local Density Approximation (LDA)

The exchange-correlation energy functional in DFT is approximated by employing local density approximation which depend on the electron density at each point in space. The exchange-correlation energy per electron at a given point $\boldsymbol{r}$ is equal to the exchange- correlation energy of the homogeneous electron gas that has the same density as the electron gas at that point is given as

$$E_{XC}[n] = \int \mathcal{E}_{XC}(\boldsymbol{r})\, n(\boldsymbol{r}) d\boldsymbol{r} \tag{2.12}$$

$\mathcal{E}_{XC}(\boldsymbol{r})$ is the exchange-correlation energy per particle of a homogeneous electron gas of charge density n. In LDA all the nonlocal dependencies of the energy functional are neglected and thus best represent for the systems, which are close to the homogeneous gas in terms of electron

density variation i.e. metallic, ionic, strongly bonded covalent etc. Due to inaccurate binding LDA underestimates the bond length and band gaps in solid [30].

2.4.2 Generalized Gradient Approximation (GGA)

In LDA the electronic density is assumed to be same throughout the space but in real system, which is not accurate. To account the non-homogeneity of the true electron density, the generalized gradient approximation (GGA) was proposed by improving LDA. According to which exchange-correlation energy is not only the functional of local density but also the functional of gradient and higher derivatives of electron density. The GGA is proposed by Perdew, Burke and Ernzerhof (PBE) [30,31].

$$E_{XC}[n] = \int n(\boldsymbol{r})\mathcal{E}_{XC}(\boldsymbol{r})[\, n(\boldsymbol{r})]F_{XC}[n(\boldsymbol{r}), \Delta n(\boldsymbol{r}), \Delta^2 n(\boldsymbol{r}), \ldots\ldots]d\boldsymbol{r} \tag{2.13}$$

Where F_{XC} is the dimensionless enhanced term involved in the modification of LDA. The GGA gives better results than LDA in reporting binding energies, atomic energy, bond lengths and bond angles. In the forthcoming section, a brief discussion of polarizable continuum modal is presented as necessary computational tools for solvent effects study.

2.5 POLARIZABLE CONTINUUM MODEL (PCM)

Continuum solvation models have been extensively used to account for the effect of solvent on molecular properties of solute [32]. It uses a dielectric medium to denote the solvent molecules without describing each solvent molecule explicitly whereas solute is described as quantum mechanical charge distribution. The dielectric medium is described by its dielectric constant, and the experimental value of the bulk solvent are chosen to be value of dielectric constant in PCM. The interactions between quantum mechanical part solute and the environment i.e. solute-solvent interactions; can be viewed into four terms which are electrostatic interaction, cavitation,

exchange-repulsion and dispersion. PCM treats the last three terms empirically as these terms have separate functional forms. In polarizable continuum model, the electrostatic interaction term between solute-solvent carries special importance. The solute molecule is treated as a charge distribution which polarizes the dielectric continuum medium. Due to the polarization, charges are induced on the surface dielectric medium which in turn polarize back the solute charge distribution [33].

In quantum mechanical framework of PCM, the solvation operator is characterized by a one-electron operator, called electrostatic potential operator, which has same form as the Coulomb operator. The effective Hamiltonian in solution can be written in terms of vacuum Hamiltonian as;

$$\hat{H}^{eff} = \hat{H} + \hat{V}^{PCM} \tag{2.14}$$

Here H is the vacuum Hamiltonian which describes an isolated molecules, and is equivalent to the Hamiltonian given by equation (2.7) and $\hat{V}^{PCM}$ is electrostatic interaction term between solute and solvent (solvent reaction potential) and given by the following relation.

$$\hat{V}^{PCM} = \sum_{k} q(\boldsymbol{s_k})\,\hat{V}(\boldsymbol{s_k}) \tag{2.15}$$

$q(\boldsymbol{s_k})$ and $\hat{V}(\boldsymbol{s_k})$ represents point charge and electrostatic potential operator on the surface tesserae at position $\boldsymbol{s_k}$. The treatment of $\hat{V}^{PCM}$ operator is sensitive due to its dependency on solute total charge density, which induces a nonlinear character in effective Hamiltonian and hence, with solute Schrodinger equation [34]. Any developed technique for isolated system is enable to solve the nonlinear equation. Thus, free energy functional G, in which nonlinearity is reflected, in the presence of PCM perturbation bears a free -energy form as;

$$G = E + \frac{1}{2}\langle\varphi|\hat{V}^{PCM}|\varphi\rangle$$

(2.16)

The solution of the Schrodinger equation gives a minimum value of this functional even if it is not the eigenvalue of the nonlinear Hamiltonian. To create the charge density inside the solvent medium the work is needed to be done by the solute, called polarization work, which is given by the difference between E and G [34]. It is also called as electrostatic interaction energy (E^{int}) due to solute-solvent polarization and given by:

$$E^{int} = \langle\varphi|\hat{V}^{PCM}|\varphi\rangle$$

(2.17)

Therefore, equation (2.16) can be written as:

$$G = E + \frac{1}{2}E^{int}$$

(2.18)

In PCM, surface charge distribution ($\sigma(\boldsymbol{s_k})$) over solute-solvent boundary is as to be discrete. This is done by discretizing boundary surface into a number of small surface elements called tesserae, (a_k). Therefore, the point charge due discrete charge distribution over tesserae of area a_k is given by;

$$q(\boldsymbol{s_k}) = \sigma(\boldsymbol{s_k})a_k$$

(2.19)

Here, is worth talking about the generation of surface mesh in PCM. The surface mesh around a solute is created by using GEPOL [33,35] algorithm. The GEPOL starts from a cavity with van der Walls radii. The cavity is generated by a set of interlocked spheres each centered on selected solute atom or molecule. In recent years, GEPOL has been significantly improved by introducing flexible tessellation or symmetry-adopted tessellations [36,37].

The solvation operator is combined into the effective Hamiltonian $\hat{H}^{eff}$, so the electronic wave function can be solved using self-consistent DFT which can be referred as self -consistent reaction field model. The classic electrostatic Poisson equation describes the electrostatic and polarization interactions among the solute molecule and the solvent molecules and establishes the dependence of electrostatic potential on the charge density and the dielectric constant:

$$\nabla^2 V^{PCM}(\boldsymbol{s_k}) = -\frac{4\pi\rho(\boldsymbol{s_k})}{\varepsilon} \tag{2.20}$$

In PCM, the portion of space in the medium occupied by the solute is referred as the molecular cavity. Onsager introduced physical meaning of a cavity in such a way that it should ignore the solvent while considering the largest possible part of the solute charge distribution . Generally, a molecular cavity is define as a set of interlocking spheres centered at each nucleus comprising the solute. In some schemes, additional spheres are used to smooth out sharp grooves. The radius of each sphere can use van der Waals radius [38] or other empirical values, such as the simplified united atomic radii, bondi, universal force field etcetera depending on the composition of solute molecule. In PCM, solvents are taken in their dilute form and the induced surface charges are calculated numerically because complex shape of cavity. The periphery of molecular cavity is molecular surface. Different types of PCM describe different formulations to examine the apparent surface charges (ASCs), viz. integral equation formalism polarizable continuum model (IEFPCM) [39,40] dielectric polarizable continuum model (DPCM) [41] conductor-like screening models (COSMO) [42] conductor-like polarizable continuum model, (CPCM) [43,44] etcetera.

2.6 COMPUTATIONAL METHODS

2.6.1 NRLMOL: Executable used in this study

The NRLMOL stand for 'Naval Research Laboratory Molecular Orbital Library' [45–49].This is a massively parallel code designed for electronic structure calculations of large

molecular systems. With NRLMOL, molecular properties such as electronic structure, density of states, optimized geometry, bond lengths, dipole moment, spin magnetic moment, harmonic vibrational frequencies, infrared and Raman spectra, electronic density, orbital density, ionization potential, electron affinity, joint density of states, optical absorption spectra, site specific polarizabilities, spin Hamiltonians etc. can be calculated. The code is based on Kohn-Sham formulation of DFT in which the electronic orbitals and eigenstates are determined using a linear combination of Gaussian atomic type molecular orbital (LCGTO) approach. We use UTEP NRLMOL codes for this study.

2.6.2 Solver Type

The solver type in used in this Conductor like Polarizable Continuum Model (CPCM), where the solvents is specified explicitly. Further in CPCM, the solvent is considered as uniform, homogeneous dielectric medium. A surface mesh is created around a quantum mechanical part i.e. solute using local PCM driver is used . The local PCM drive is developed in the UTEP Electronic Structure Lab, represented as PCM(O), which is interfaced in (DFT). All the calculations are spin polarized and used conductor like PCM.

2.6.3 Computational Approach

The calculations are performed using polarizable continuum model incorporated in density functional theory at all electron level using Perdew-Burke-Ernzerhof exchange correlation functional. All the calculations reported in this work are performed using UTEP NRLMOL code with default NRLMOL Gaussian basis set.

The computation work in this thesis involves the calculation of ground and excited DFT energies in the solvents of variant polarity. With these solvents, a surface mesh is created around the endohedral fullerene molecular complexes. To create surface mesh around a quantum

mechanical part of system of interests, local PCM driver is used. Once the system is running with a code, developed in UTEP electronic structure group, in this PCM driver, the output is fed into ground state polarization and total energy calculation using UTEP NRLMOL code in the Kohn-Sham DFT level. Then calculation are making into excited states.

A method, called perturbative delta self-consistent, had been developed some years back in our lab that allows efficient calculations of the electronic excitations by employing perturbation theory. By using this method, any excitations can be calculated by enforcing an orthogonality between the ground state total wavefunction and excited state total wavefunction. These wavefunctions are composed as single Slater determinants form Kohn-Sham orbitals. The accurate calculations on charge transfer excitations [20,22] had made on a set of TCEN families along with other donor-acceptor complexes, which benchmarked this method as an accurate method for charge transfer calculation for big clusters. NRLMOL is based on the Kohn-Sham (Schrödinger equation of a system of non-interacting particles generating the same potential as any system of interacting particles) formulation of DFT and solves the Kohn-Sham equations by expressing the Kohn-Sham wave functions as a linear combination of the Gaussian orbitals. The default basis set of the code is particularly optimized for the Perdew-Burke-Ernzerhof (PBE) exchange-correlation energy functional within the Generalized Gradient Approximation (GGA) [49]. All the calculations are done at the all electron level and all the systems have a closed shell electronic configuration.

Due to the huge size of the complexes studied in this work the quantum chemical methods such as configuration interaction (CI) or multi reference CI cannot be applied to run their excited states calculation. For a supra molecular systems having atoms more than 100 atoms, the excited state phenomena, like optical spectra, can be studied by using time dependent density functional theory (TDDFT) in its linear response formulation. However, for the determination of donor-acceptor conjugates' excitation energies, TDDFT is not that useful because of the failure in

describing charge transfers excitations. By imposing system dependent constraints and tricks [20], TDDFT can be made useful. Thus a formulation, in which constrained is applied to describe the lowest charge transfer excitations of the complex system, called constrained formalism of DFT enables us to describe charge transfer excitations. This approach establishes a constraining potential to enforce electron density's localization [19,50]and provides only the lowest excited states.

2.6.4 Solvents Used and DFT-PCM Method

The macroscopic properties for the built-in list of solvents used in this study are given in the following table 2.1.

Table 2.1:Static and optical permittivity and probe radius for solvent used

S.N.	Name of Solvent	Static Permittivity ($\boldsymbol{\varepsilon_s}$)	Optical Permittivity ($\boldsymbol{\varepsilon_\infty}$)	Probe Radius ($\boldsymbol{r_{probe}}$)
1	Water	78.39	1.776	1.385
2	Acetone	20.7	1.841	2.38
3	Toluene	2.379	2.085	2.82

These solvents are so choose that the static permittivity decreases on going form water (78.39) to toluene (2.379). The logic of choosing these solvent is that how dipole moment, polarization energy, and charge transfer occur on moving from polar solvents to non-polar solvents.

To analyze the environmental effect on molecular system PCM is used. In all PCM models, the representation of surface charge distribution over the solute-solvent boundary is discrete. The surface is discretized into N surface elements, called tesserae and are characterize by their position and surface area. In fact, in PCM, discretization of the surface is equivalent to the charge discretization, which is necessary for the generation of surface mesh. In this work, surface mesh are generated using GEPOL, which starts from a cavity generated by interlocking spheres centered

on a particular solute atom of interest [34]. We set the area of a tesserae equal to 0.2, minimum radius of sphere to be added equal to 100, built-in radii is UFF (universal force field) and the type of solver is the conductor-like polarizable continuum model (CPCM). Within this parameters the PCM is implemented in DFT framework. In DFT model, the ground state electron density plays a significant role for the complete information of electronic system. The same holds for DFT-PCM formulation, with addition of perturbation term due to solute and solvent interaction, which can be dumped in to the effective potential so that we know solve KS equations exactly as we do for an isolated molecular system. Also, we can generalize the concept in terms of the Hamiltonian, which is the sum of gas phase DFT Hamiltonian and electrostatic interaction potential between solute and the solvent environment. So, the effective Hamiltonian in DFT-PCM formulation is simply the perturbed Hamiltonian due to the medium in which molecular system resides.

2.6.5 Primitive Gaussian and Functions

The number of primitive Gaussians, S-type, P-type and D-type functions as well as the range of the exponents for individual atoms used in this work are listed in the table below. This basis set resulted in total 4723 basis functions for $Sc_3N@C_{80}$–ZnPc, 4715 for $Sc_3N@C_{80}$–H_2Pc , 2973 for $Sc_3N@C_{80}$, 1750 for ZnPc and 1742 for H_2Pc.

Table 2.2: The numbers of S-, P-, D-type contracted functions, number of primitive Gaussians used for each atom.

Atoms	S-type functional	P-type functional	D-type functional	No. of bare Gaussians/primitives
Carbon	5	4	3	12
Nitrogen	5	4	3	13
Hydrogen	4	3	1	6
Scandium	7	5	4	19

Zinc	7	5	4	20

All the calculations start with the optimization of geometry of the systems of interest under study. Geometry optimization indicates the rearrangement of the positions of individual atoms in such a way that the total force acting on each atom becomes null. An optimized system possessed a minimum energy and is said to be minimum energy state.

Chapter 3: Results and Discussion

The isolated donors and acceptors utilized in this work are triscandium nitride C_{80} fullerene ($Sc_3N@C_{80}$), Phthalocyanine ($(C_8H_4N_2)_4H_2$), (denoted as H_2Pc) and Zinc Phthalocyanine ($(C_8H_4N_2)_4Zn$) (denoted as ZnPc) are described in chapter 1. The sovent used are water, acetone, and toluene which are given in Table 2.1. In this section, the result of calculations based on these donor-acceptor pairs on gas phase and in the solvent environment will be discussed . All the calculations are spin polarized state and used local polarization continuum model (PCM) which is implemented in DFT using UTEP NRLMOL suite of codes.

3.1 GROUND STATE CALCULATIONS

All the calculations discussed in this sub-section are performed by using Density Functional Theory in gaseous medium. First of all, ground state energies of H_2Pc, ZnPc, $Sc_3N@C_{80}$, $Sc_3N@C_{80}$–H_2Pc and $Sc_3N@C_{80}$–ZnPc are calculated by taking the optimized geometries of those molecules and gas phase electronic properties like electronic affinity, ionization potential, dipole moments are computed. All the calculations are performed in spin-polarized states. The table (3.1) below shows total ground state energies for the systems in their net charged state of ±1 and 0 (ionic and neutral state).

Table 3.1: Ground state energies of systems of interests and their components

	Ground State Energies (eV)		
	Net Charge		
Systems	**+1**	**0**	**-1**
H_2Pc	- 45355.27	-45361.67	-45363.80
ZnPc	-93739.33	-93745.68	-93747.76
$Sc_3N@C_{80}$	-146461.83	-146468.51	-146471.00
$Sc_3N@C_{80}$–H_2Pc	-191823.79	-191829.96	-191832.60
$Sc_3N@C_{80}$–ZnPc	-240207.77	-240213.89	-240216.51

Based on DFT calculations, the vertical ionization potential, vertical electron affinity, quasiparticle gap, ground state HOMO–LUMO gap and Fermi level of the $Sc_3N@C_{80}$, $Sc_3N@C_{80}$–H_2Pc and $Sc_3N@C_{80}$–ZnPc as well as H_2Pc and ZnPc are tabulated in the Table below.

Table 3.2: Ground state electronic properties of system interests in gas phase

Systems	vIP(eV)	vEA(eV)	QP (eV)	Homo-Lumo gap (eV)
ZnPc	6.35	2.08	4.28	1.39
H_2Pc	6.39	2.13	4.26	1.38
$Sc_3N@C_{80}$	6.63	2.48	4.14	1.46
$Sc_3N@C_{80}$–H_2Pc	6.17	2.64	3.52	1.32
$Sc_3N@C_{80}$–ZnPc	6.12	2.62	3.50	1.14

The vertical ionization potential, which is obtained by the energy difference of optimized cation and the neutral atom, gives the tendency to lose electron(s) form a neutral atom, while the vertical electron affinity gives a capacity of neutral atom to acquire an electron(s). It is seen that the both of these complexes $Sc_3N@C_{80}$–H_2Pc and $Sc_3N@C_{80}$–ZnPc exhibit similar vIP and vEA. It implies that both of these D-A pair has almost same capacity to acquire or lose an electron. The slight greater value of the vertical ionization potential of complex $Sc_3N@C_{80}$–vH_2Pc (6.1707 eV) than $Sc_3N@C_{80}$–ZnPc (6.120 eV) may be due the slight greater value of vIP of isolated H_2Pc (6.3936 eV) than ZnPc (6.354 eV). On the other hand, we have seen that vertical electron affinity of both isolated H_2Pc (2.1336 eV) and complex $Sc_3N@C_{80}$–H_2Pc (2.6451 eV) are respectively greater than isolated ZnPc (2.078 eV) and complex $Sc_3N@C_{80}$–ZnPc (2.616 eV). Therefore, it can be concluded that ZnPc gives electrons fairly well to fullerene cage than H_2Pc because of having less ionization potential and more electron affinity. In addition the electron affinity ($\sim$ 2.49 eV) of $Sc_3N@C_{80}$ fullerene is greater than electron affinities of both the H_2Pc and ZnPc, which verifies that fullerene cages tend to accept electrons (acceptor) while ZnPc and H_2Pc serve as donor in $Sc_3N@C_{80}$–H_2Pc and $Sc_3N@C_{80}$–ZnPc complexes. However, due to having almost same values

of vEA and vIP, fullerenes may reverses its characteristics by donating electrons in higher excitations to ZnPc or H_2Pc.

The quasiparticle gap is calculated by the difference between vertical ionization potential and vertical electron affinity. It is almost same for both of these charge transfer complexes with the values of 3.5256 eV and 3.504 eV respectively for $Sc_3N@C_{80}$_H_2Pc and $Sc_3N@C_{80}$_ZnPc.

Dipole moment is a measure of the net molecular polarity and tells about the charge separations in a molecule. For non-polar molecules, in which center of positive and negative charges lie in the same plane, its value is zero. On the other hand, for polar molecules center of -ve and +ve charges do not coincide and they have dipole moment. The measured dipole moments of $Sc_3N@C_{80}$, $Sc_3N@C_{80}$–H_2Pc and $Sc_3N@C_{80}$–ZnPc are about 0.25D, 1.4D and 0.32D respectively.

The optical gap, which is a measure of HOMO to LUMO excitation energy, for these systems are found to be 1.52eV, 1.77 eV and 2.15 eV respectively for $Sc_3N@C_{80}$, $Sc_3N@C_{80}$–H_2Pc and $Sc_3N@C_{80}$–ZnPc.

All of the above calculation then compared with the previously studied data, which are reported in Amerikheriabadi et al. [12] and Basurto et al. [11] and the results obtained agree precisely. As this experiment is done in the same experimental setting and computed by using same suites of code, reported values are taken as benched mark, and will borrow whenever needed in the subsequent results discussion. Herein, in the forthcoming sections we discuss the solvent effect in the ground and charge transfer excited states properties of the electron-donor-acceptor pairs using DFT-PCM approach.

3.2 SOLVENT EFFECT ON THE ELECTRONIC STRUCTURE OF THE DONOR ACCEPTOR COMPLEXES

Due to polarization the gas phase Hamiltonian is perturbed and there occurs changes in the electronic properties of materials. Here in this section, various ground and charge transfer excited states properties of system of interests in three different solvents environment are studied and presented. The solvents taken are water, acetone and toluene with static permittivity 78.39, 20.7 and 2.379 respectively.

3.2.1 Ground State Calculations

As stated earlier sections, the orientation of molecular complexes studied in this dissertation work are co-facial, which are bound together by weak van der Waals force. It is also assumed that the entrapped tri-scandium nitride unit the fullerene cage of dyads does not produce any significant changes in the electronic properties like charge transfer [11]. As reported in earlier section that, the binding energy of complex with zinc is more than complex with free base phtalocyanine. It indicates that Sc_3NC_{80}–ZnPc is more stable than Sc_3NC_{80}–H_2Pc. Using CPCM, ground state calculations are made on DFT. The total energy of isolated Sc_3NC_{80} and two complexes Sc_3NC_{80}–H_2Pc and $Sc_3NC@_{80}$–ZnPc are computed. The inclusion of solvents result the polarization energy in the output of DFT calculations. The total DFT energy of the dyads Sc_3NC_{80}–H_2Pc and $Sc_3N@C_{80}$–ZnPc in isolation (i.e. gas) are found to be -191829.96 eV and -240213.90 eV respectively. The table 3.3 depicts the total energies of these dyads due to solvents effect and comparison of the gas phase results.

Table 3.3: Total and interaction energies of systems of interests in water, acetone and toluene

Systems	Total DFT energy in solvents (G) (in eV)	Solute-Solvent Interaction energy (E^{int}) (in eV)	$\boldsymbol{Egas, PCM}$ = $(\boldsymbol{G - \frac{1}{2}E^{int}})$ (in eV)	$\boldsymbol{\Delta E = E_{gas,DFT} - E_{gas,PCM}}$ (in eV)

Solvent as Water				
$Sc_3N@C_{80}$–ZnPc	-240214.19	-0.35	-240214.02	0.12
$Sc_3N@C_{80}$–H_2Pc	-191830.19	-0.27	-191830.06	0.10
Solvent as Acetone				
$Sc_3N@C_{80}$–ZnPc	-240214.18	-0.34	-240214.01	0.11
$Sc_3N@C_{80}$–H_2Pc	-191830.18	-0.26	-191830.05	0.09
Solvent as Toluene				
$Sc_3N@C_{80}$–ZnPc	-240214.06	-0.18	-240213.97	0.07
$Sc_3N@C_{80}$–H_2Pc	-191830.08	-0.14	-191830.01	0.05

From the above table we can draw an important conclusion that PCM implemented in DFT using UTEP NRLMOL codes adequately accounts the polarization effects produced due to the inclusion of solvents. A slight difference in ΔE might due to solvent modal itself because of the following reasons. Firstly, PCM assumed that the solvent as continuum in which interaction between solute and solvents take place implicitly. That is the modal treats solvent as a continuous medium instead of considering molecular details each solvent molecule. Secondly, in our calculation we use conductor like polarizable continuum modal (CPCM) which has some drawbacks. If we neglect small errors present in calculation the, PCM–DFT modal gives the exact solution of perturbed Schrodinger equation given by effective Hamiltonian in continuum medium.

Moreover, the magnitude of interaction polarization energy due to toluene as a polarizable medium is least among the rest two solvents listed in the table. Its concludes that the solvents having more static permittivity i.e. polaric solvent has more interaction polarization energy while those solvents which are non-polar in nature have less interaction polarization energy. It might be due to the reason that for the charge distribution around the solute-solvent interface, less more is needed to be done in polar-solvent environment due to their internal electric field. On the other hand, for non-polaric environment, the negative and positive charge coincide at same point so there is no internal electric field in them and less work is necessary to create charge distribution on the solute-solvent interface.

Further, while comparing the interaction energies of these two complex, $Sc_3N@C_{80}$–H_2Pc has less value in each of the three solvents studied than $Sc_3N@C_{80}$–ZnPc. Its supports that $Sc_3N@C_{80}$–ZnPc is more favorable candidate as concluded by Fatemeh et al. [12] for charge transfer than $Sc_3N@C_{80}$–H_2Pc because of having greater reorganization energy.

The DFT-PCM calculated vertical ionization potential (vIP), electron affinity (vEA), qusiparticle gap(QPG), HOMO–LUMO gap, optical gap (OG), and Fermi-level of these system of interests in three different solvents viz. water, acetone and toluene are reported in the following tables below.

Table 3.4:Ground state vertical ionization potential, electronic affinity, quasiparticle gap, HOMO-LUMO gap, and Fermi-level values of systems of interest in water

Systems	vIP(eV)	vEA(eV)	Quasiparticle Gap(eV)	HOMO-LUMO gap(eV)	Opticael Gap(eV)
$Sc_3N@C_{80}$–ZnPc	5.26	3.63	1.64	1.23	1.68
$Sc_3N@C_{80}$–H_2Pc	5.33	3.67	1.66	1.34	1.49

Table 3.5:Ground state vertical ionization potential, electronic affinity, quasiparticle gap, HOMO-LUMO gap, and Fermi-level values of systems of interest in acetone

Systems	vIP(eV)	vEA(eV)	Quasiparticle Gap(eV)	HOMO-LUMO gap(eV)	Optical Gap(eV)
$Sc_3N@C_{80}$–ZnPc	5.30	3.59	1.71	1.22	1.72
$Sc_3N@C_{80}$–H_2Pc	5.36	3.63	1.73	1.34	1.49

Table 3.6:Ground state vertical ionization potential, electronic affinity, quasiparticle gap, HOMO-LUMO gap, and Fermi-level values of systems of interest in toluene

Systems	vIP(eV)	vEA(eV)	Quasiparticle Gap(eV)	HOMO-LUMO gap(eV)	Optical Gap(eV)
$Sc_3N@C_{80}$–ZnPc	5.62	3.20	2.42	1.18	1.56
$Sc_3N@C_{80}$–H_2Pc	5.44	3.53	1.91	1.33	1.87

From above tables, it is seen that the vertical ionization potentials of these complexes in solvents are found to be reduced significantly than the reported values of 6.12 eV and 6.17 eV respectively for $Sc_3N@C_{80}$–ZnPc and $Sc_3N@C_{80}$–H_2Pc in gas phase DFT calculations [51]. On the other hand, the vertical electronic affinity of the complexes found to be increased in solvents than in gas. These two facts conclude that in solutions, the donor parts tend to give electron(s) more readily while and acceptor parts show greater tendency to acquire electrons than in gas phase. If we compare the calculated values of vIP and vEA in solvents, it can be seen that the value of vIP increases with decreasing permittivity while vEA decreases in such a way that the quasiparticle gap in toluene is maximum and minimum in water.

It is interesting to figure out that the quasiparticle gap in solution is reduced by more or less about 50% for each of solvents taken. The reported values of quasiparticle gap for $Sc_3N@C_{80}$–ZnPc and $Sc_3N@C_{80}$–H_2Pc in isolated environment were 3.50 eV and 3.53 eV respectively. In contrast, the QP values for $Sc_3N@C_{80}$–ZnPc in water, acetone and toluene as environment are found to be 1.64 eV, 1.72 eV and 2.42 eV respectively and corresponding QP values in those solvents for $Sc_3N@C_{80}$–H_2Pc are 1.66 eV, 1.73 eV, 1.91 eV. The quasiparticle gap signifies the energy needed for the addition or the subtraction of electrons from neutral atoms in their ground state. In solvents, charge transfer takes place fairly easily than in gas which might due to the polarization effect. Further, the QP gap of $Sc_3N@C_{80}$–ZnPc complex in solution, in general, is slightly less than that of $Sc_3N@C_{80}$–H_2Pc except in toluene.

The energy gap in the gas phase of these two complexes $Sc_3N@C_{80}$_ZnPc and $Sc_3N@C_{80}$_H_2Pc in their ground states, calculated in PBE level of DFT, were 1.14 eV and 1.32 eV respectively. Although, the energy gap so calculated underestimates fundamental band gap due to missing derivative discontinuity and unable to give optical gap due missing particle-hole interactions [52], it is worth talking the effect of solvents for the sake of comparison. It is found that the HOMO-LUMO gap for $Sc_3N@C_{80}$_ZnPc in solution increases slightly while for $Sc_3N@C_{80}$_H_2Pc almost stays fixed. This shows that the potential due to the solvent is not strong enough to make significant changes in the eigenvalues.

The ground state dipole moments for isolated $Sc_3N@C_{80}$ as well as D/A dyads $Sc_3N@C_{80}$–H_2Pc and $Sc_3N@C_{80}$–H_2Pc are computed in DFT PBE level which are presented the table (3.7) as shown.

Table 3.7: Dipole Moments in Debye (D)

Systems / **Medium**	**$Sc_3N@C_{80}$**	**$Sc_3N@C_{80}$–H_2Pc**	**$Sc_3N@C_{80}$–ZnPc**
Gas(vacuum)	0.25	1.40	0.32
Water	0.49	0.71	0.92
Acetone	0.47	0.75	0.86
Toluene	0.35	1.10	0.44

The molecular dipole moment is important for polarization of dielectric (medium) which can be used to in charge storing devices like capacitors. The DFT calculated value of dipole moments in gas for $Sc_3N@C_{80}$–H_2Pc is 1.4D and .032 D for $Sc_3N@C_{80}$–ZnPc. For isolated $Sc_3N@C_{80}$, the value of dipole moment in gas is 0.25 D, but when in solutions its calculated value found to changed significantly. In water, it is increased by 0.24D, while in acetone and toluene by 0.22 D and 0.10 D respectively. It might demonstrate polarization effect is more in polar molecules

like water than non-polar molecules. Similarly, in the case of $Sc_3N@C_{80}$–ZnPc the dipole moment is found to be increase in solvent of increasing polarity. In contrast, for $Sc_3N@C_{80}$–H_2Pc, DFT–PCM calculation showed that dipole moment is decreasing with increasing polarity of solvent used, while the gas phase value of dipole moment is maximum. It might indicate that $Sc_3N@C_{80}$–H_2Pc polarizes more itself than in solutions. Another important conclusion from the dipole moment study can be drawn about the molecular ability to accept electrons, which is also referred in terms of electronegativity. From the our calculations, it is shown that the $Sc_3N@C_{80}$–H_2Pc is more electronegative than $Sc_3N@C_{80}$–ZnPc in non-polar solvents while polar solvents increased electronegativity of $Sc_3N@C_{80}$–ZnPc in comparison to that of $Sc_3N@C_{80}$–H_2Pc.

3.2.2 Density of States

The number of states per unit energy range is expressed in terms of density of states (DOS). The DOS plots give the probability of getting orbitals for occupation in a particular energy. A high value of DOS at some particular energy means that there are many available states for occupation while zero signifies no states are occupied for that particular value of energy. The DOS plots for the systems of interest in the respective solvents are given in the following curves as shown.

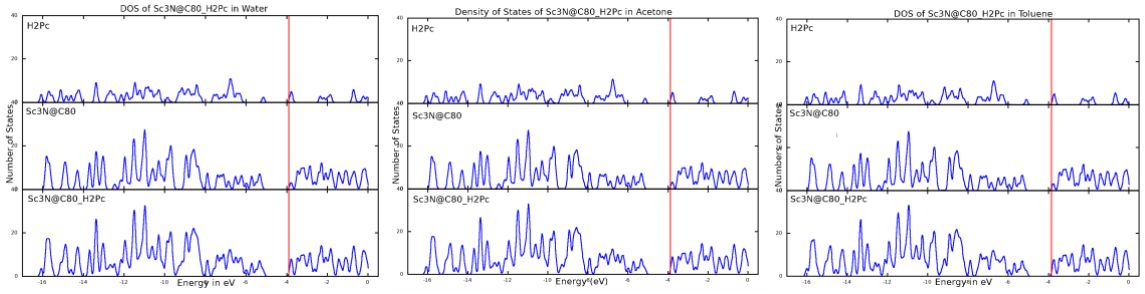

(a) (b) (c)

Figure 3.1: Density States Plots of $Sc_3N@C_{80}$–H_2Pc in (a) Water, (b) Acetone and (c) Toluene

In above DOS plots, the available state for a particular energy is same in all cases. The only difference is the position of fermi level. The red lines indicate the position of fermi levels. The

states to the left of fermi level are occupied while those at right are unoccupied. The DOS plots system in solvents are basically the DOS plots of the system with shifted fermi level energy value. In $Sc_3N@C_{80}$–H_2Pc, there are few unoccupied states in phthalocyanine part and several closely spaced unoccupied states in fullerene part of the complex. In this complex, the HOMO is localized on H_2Pc while LUMO rests on $Sc_3N@C_{80}$.

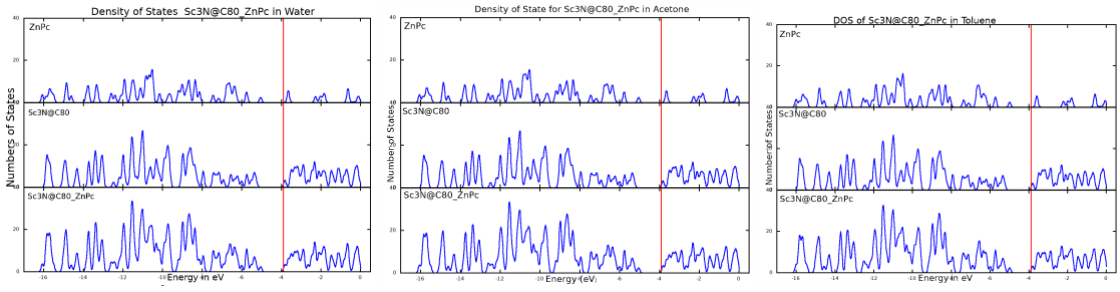

(a) (b) (c)

Figure 3.2: Density States Plots of $Sc_3N@C_{80}$–ZnPc in (a)Water, (b)Acetone and (c)Toluene

Similarly in the case $Sc_3N@C_{80}$_ZnPc, there are again a very few sparsely located unoccupied orbitals in Zn-phthalocyanine part of the complex, while densely occupied states are located at its HOMO side. In the fullerene part, there are many low-lying unoccupied states close to each other the LUMO while HOMO contained high peaked occupied states.

3.3 CHARGE TRANSFER EXCITATIONS

An essential factor that decides the efficiency of the photovoltaic device is the open-circuit voltage which is related to the charge transfer excitation energy. The charge transfer triplet and singlet excitation energies of some low-lying excited states of both the electron-donor-acceptor pairs in water, acetone and toluene are computed using perturbative delta-SCF method [19,22] which are listed in the following tables. In this work, calculations of the excited states related to the transitions to the lowest four LUMOs are made from HOMO, HOMO-1and HOMO-2 of the D/A complexes. The singlet excited state energy is estimated by a method called Ziegler-

Rauk [25] given by equation(1.5). All the listed transitions are optically permitted. It is reported in Fatemeh et.al [12] that the LUMO is nondegenerate orbital in $Sc_3N@C_{80}$ while next higher empty orbitals are double or nearly degenerated.

3.3.1 Orbital Densities

Orbital densities of the orbital involved in the excitation are shown in 3.3. Assuming small changes in the orbital densities upon the excitation, it shows the localization of the orbitals and also qualitative analysis on the transition Pure charge transfer state represents the charge transfer purely from donor part of molecular complex to the acceptor part. Local excitation represents donor to donor or acceptor to acceptor transitions within the molecular complexes, while the partial charge transfer can occur when the orbital density is spread over both donor and acceptor parts of complex. In addition, the reverse charge transfer represents charge transfer from acceptor to the donor part of molecular complex. The orbital densities of active orbitals for transitions from HOMO, HOMO-1 and HOMO-2 to the lowest four LUMOs of $Sc_3N@C_{80}$_H_2Pc and $Sc_3N@C_{80}$_ZnPc complex in vacuum figures below.

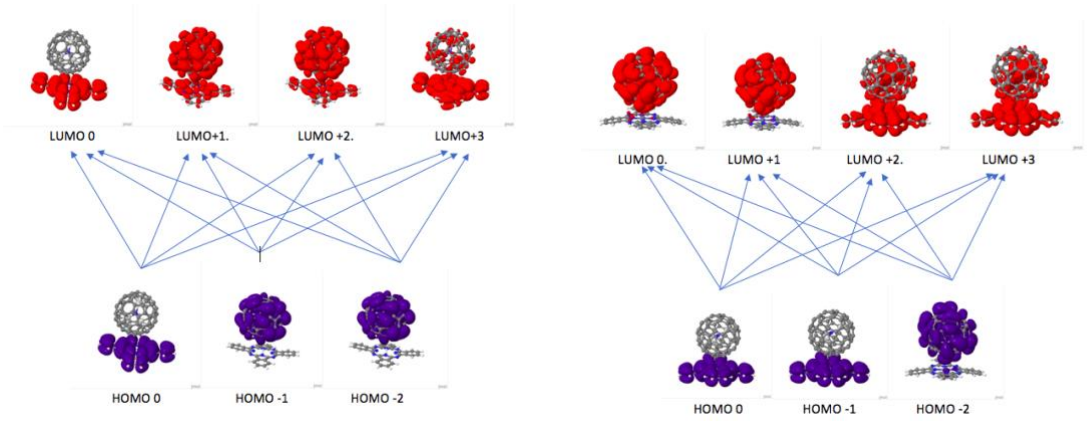

(a) (b)

Figure 3.3: Transitions from HOMO, HOMO-1 and HOMO-2 to the lowest four LUMOs of (a) $Sc_3N@C_{80}$–H_2Pc and (b) $Sc_3N@C_{80}$–ZnPc complex in vacuum (gas).The orbitals densities of active orbitals are shown.

Form the figure, we have seen that, the HOMO-LUMO transition in $Sc_3N@C_{80}$–H_2Pc represents local charge transfers state, while HOMO-1–LUMO and HOMO-2–LUMO in it transitions represents reverse charge transfer state. There are no pure charge transfer states in $Sc_3N@C_{80}$–H_2Pc which excitations are made in vacuum but it is observed in $Sc_3N@C_{80}$–ZnPc. The transitions HOMO–LUMO, HOMO–LUMO+1, HOMO-1–LUMO and HOMO-1–LUMO+1 in (b) are the pure charge states. The majority of transitions for both complexes in gas are partial charge transfer states.

3.3.2 Orbital Densities and Charge Transfer Excitations in Water

The orbital densities of active orbitals for Transitions from HOMO, HOMO -1 and HOMO-2 to the lowest four LUMOs of $Sc_3N@C_{80}$–H_2Pc and $Sc_3N@C_{80}$–ZnPc complex in water as solvent are shown figures below. The numbers on the transitions showing the excitation energies in electron volts.

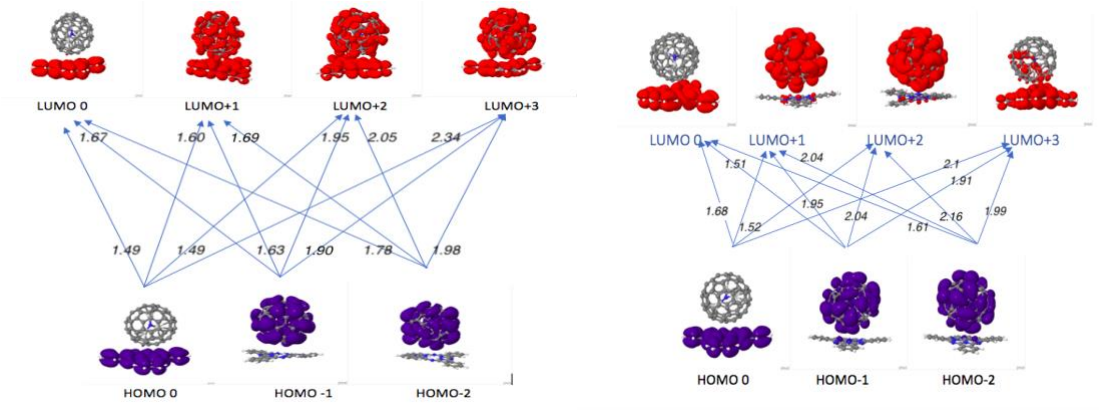

(a) (b)

Figure 3.4: Transitions from HOMO, HOMO-1 and HOMO-2 to the lowest four LUMOs of (a) $Sc_3N@C_{80}$–H_2Pc and (b) $Sc_3N@C_{80}$–ZnPc complex in water. The orbitals densities of active orbitals are shown. The number on the line showing transition represent CT excitation energy values.

The calculated values of charge transfer excitation energy of the molecular complexes when water is used as solvent are reported the table below.

Table: 3.8: Charge transfer excitation energies in water. *, **, and *** in the column of singlet excitation energy denote the local, partial and reverse charge transfer states respectively.

Transitions	$Sc_3N@C_{80}$–ZnPc(in eV)		$Sc_3N@C_{80}$–H_2Pc(in eV)	
	Singlet	Triplet	Singlet	Triplet
HOMO–LUMO	1.68*	1.64	1.49*	1.27
HOMO–LUMO +1	1.52	1.28	1.60**	1.44
HOMO–LUMO+2	1.52	1.28	1.49**	1.35
HOMO–LUMO+3	2.1**	2.04	2.34**	2.24
HOMO-1–LUMO	1.51***	1.47	1.67***	1.65
HOMO-1–LUMO+1	1.95*	1.93	1.63**	1.59
HOMO-1–LUMO+2	2.04*	2.04	1.95**	1.93
HOMO-1–LUMO+3	1.91**	1.87	1.90**	1.86
HOMO-2–LUMO	1.61***	1.55	1.78***	1.72
HOMO-2–LUMO+1	2.04*	2.02	1.69**	1.67
HOMO-2–LUMO+2	2.16*	2.14	2.05**	2.03
HOMO-2–LUMO+3	1.99**	1.93	1.98**	1.92

In water, for $Sc_3N@C_{80}$_ZnPc, the singlet CT excitation energy ranges from 1.51eV to 2.16 eV for the transitions form HOMO, HOMO-1 and HOMO-2 to the lowest four LUMOS. It has been observed that HOMO-LUMO+1 and HOMO-LUMO+2 and have same excitation energy which is 1.52eV. These state are called degenerated states. Similarly, degeneracy also appears in the transitions HOMO-2–LUMO+1 and HOMO-1–LUMO+2, while HOMO-1–LUMO is nearly degenerated with the transitions HOMO–LUMO+1 and HOMO–LUMO+2. The three most significant CT excitation energies in $Sc_3N@C_{80}$–ZnPc are 2.16eV, 2.10 eV and 2.04 eV which correspond to the transitions HOMO-2–LUMO+2, HOMO–LUMO+3 and HOMO-2–LUMO+1.

In case of $Sc_3N@C_{80}$–H_2Pc, the largest value of CT excitation energy among observed twelve transitions is 2.34 eV corresponding to transition HOMO–LUMO+3, while lowest among them is 1.49 eV corresponding to the transitions HOMO–LUMO and HOMO–LUMO+2. Among $Sc_3N@C_{80}$–ZnPc and $Sc_3N@C_{80}$–H_2Pc, the former one has more significant transition energies despite most charge transfer excitation energy 2.34 eV observed in transition from HOMO to LUMO+3 in the later one.

The transitions HOMO–LUMO+1 and HOMO–LUMO+2 are pure CT states in $Sc_3N@C_{80}$–ZnPc while these are absent in $Sc_3N@C_{80}$–H_2Pc. The transitions HOMO-1–LUMO and HOMO-2–LUMO for both complexes in water are reverse CT state where charge move form fullerene to corresponding donors i.e. ZnPc or H_2Pc. The majority of transitions in the complex with ZnPc in water show local CT state whereas these kinds of transitions also are absent in dyads with H_2Pc. For the complex with H_2Pc in water, most of the transitions are partial CT states. The pure CT states with high value of excitation energy are important for photo-induced current to be high. Thus, $Sc_3N@C_{80}$–ZnPc in water is more selective than $Sc_3N@C_{80}$–H_2Pc complex for OPVs.

3.3.3 Orbital Densities and Charge Transfer Excitations in Acetone

The orbital densities of active orbitals for Transitions from HOMO, HOMO-1 and HOMO-2 to the lowest four LUMOs of $Sc_3N@C_{80}$–H_2Pc and $Sc_3N@C_{80}$–ZnPc complexes in acetone as solvent are shown in a figure given below.

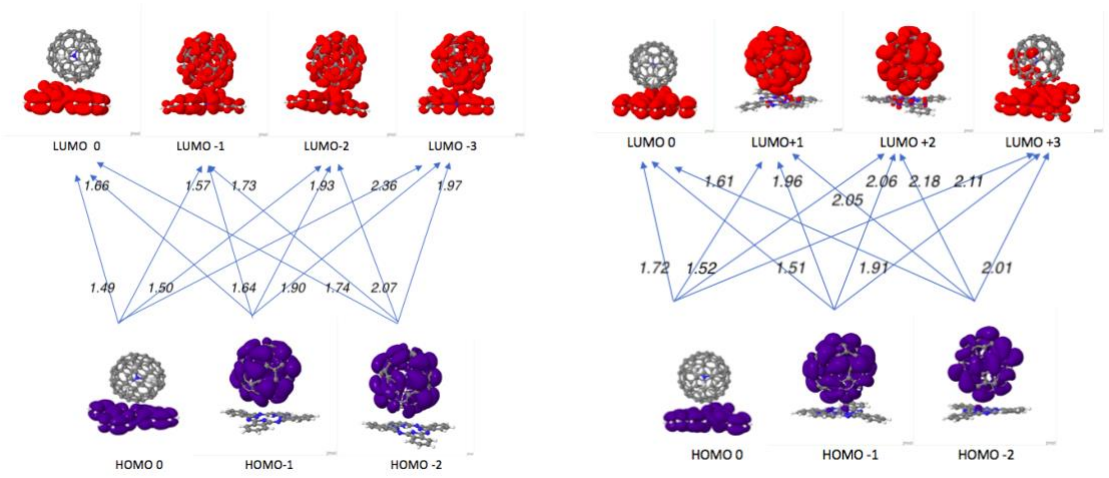

(a) (b)

Figure 3.5: Transitions from HOMO , HOMO-1 and HOMO-2 to the lowest four LUMOs of (a) $Sc_3N@C_{80}$–H_2Pc and (b) $Sc_3N@C_{80}$–ZnPc complex in Acetone. The orbitals densities of active orbitals are shown. The number on the line showing transition represent CT excitation energy values

Table: 3.9: Charge transfer excitation energies in Acetone. *, **, and *** in the column of singlet excitation energy denote the local, partial and reverse charge transfer states respectively.

Transitions	$Sc_3N@C_{80}$–ZnPc(in eV)		$Sc_3N@C_{80}$–H_2Pc(in eV)	
	Singlet	Triplet	Singlet	Triplet
HOMO–LUMO	1.72*	1.66	1.49 *	1.29
HOMO–LUMO +1	1.52	1.28	1.57**	1.43
HOMO–LUMO +2	1.52	1.28	1.50**	1.34
HOMO–LUMO +3	2.11**	2.03	2.36**	2.26
HOMO-1–LUMO	1.51***	1.47	1.66***	1.64
HOMO-1–LUMO +1	1.96*	1.94	1.64**	1.62
HOMO-1–LUMO +2	2.06*	2.06	1.93**	1.91
HOMO-1–LUMO +3	1.91**	1.87	1.9**	1.86
HOMO-2–LUMO	1.61***	1.55	1.74***	1.72
HOMO-2–LUMO+1	2.05*	2.03	1.73**	1.69

HOMO-2–LUMO+2	2.18*	2.16	2.07**	1.97
HOMO-2–LUMO+3	2.01**	1.93	1.97**	1.93

The above table depicts the calculated values of CT excitation energies for different transition when acetone is using as solvent. In the case of acetone as solvent, the maximum value of CT excitation energy 2.18 eV is computed for $Sc_3N@C_{80}$–ZnPc in the transition from HOMO-2–LUMO+2 while the lowest is observed in the HOMO-1–LUMO transition with CT excitation value 1.51 eV. When the experiment is performed for $Sc_3N@C_{80}$–H_2Pc in acetone, the largest value of CT excitation energy among observed transitions is 2.36 eV corresponding to the transition HOMO–LUMO+3, while lowest corresponds to the transition from HOMO–LUMO and energy value is found to be 1.49 eV. Further, just like water as solution, majority of the transitions for the complex $Sc_3N@C_{80}$–ZnPc in acetone have greater values of excitation energy than the corresponding transitions in Sc3N@C80–H2Pc, thereby indicating this complex a better CT complex over the complex with H_2Pc.

The orbitals that represent pure, partial, local and inverse CT are indicated in the excited state energy values in the above table. Similar to water, we have observed only two pure CT excitations HOMO–LUMO+1 and HOMO–LUMO+2 with excitation energy 1.52 eV each for $Sc_3N@C_{80}$–ZnPc while pure CT are missing for $Sc_3N@C_{80}$–H_2Pc. Likewise, majority of transitions in the complex with H2Pc have display partial CT. Furthermore, we observed that the complex with ZnPc have majority of greater CT excitation energies than the complex with H_2Pc. Therefore, the complex having Zn is more effective to use as an active material in OPVs.

3.3.4 Orbital Densities and Charge Transfer Excitations in Toluene

The orbital densities of active orbitals for Transitions from HOMO, HOMO-1 and HOMO-2 to the lowest four LUMOs of $Sc_3N@C_{80}$–H_2Pc and $Sc_3N@C_{80}$–ZnPc molecular complexes in toluene as solvent are shown in a figure given below.

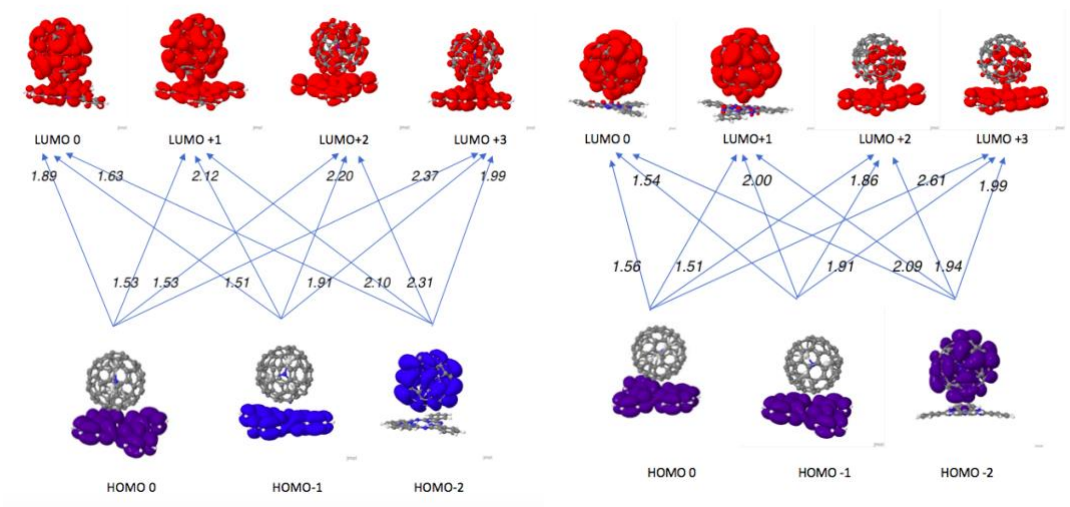

(a) (b)

Figure 3.6: Transitions from HOMO , HOMO -1 and HOMO-2 to the lowest four LUMOs of (a) $Sc_3N@C_{80}$–H_2Pc and (b) $Sc_3N@C_{80}$–ZnPc complex in toluene. The orbitals densities of active orbitals are shown. The number on the line showing transition represent CT excitation energy values.

The table below gives the CT excitation energy for the complexes when toluene as acting as continuum medium. The pure, local, partial and inverse CT states are also indicated.

Table: 3.10: Charge transfer excitation energies in toluene. *, **, and *** in the column of singlet excitation energy denote the local, partial and reverse charge transfer states respectively.

Transitions	$Sc_3N@C_{80}$–ZnPc (in eV)		$Sc_3N@C_{80}$–H_2Pc (in eV)	
	Singlet	Triplet	Singlet	Triplet
HOMO–LUMO	1.56	1.44	1.89**	1.85

HOMO–LUMO +1	1.51	1.29	1.53**	1.29
HOMO–LUMO +2	1.51**	1.31	1.53**	1.29
HOMO–LUMO +3	2.61**	2.47	2.37**	2.31
HOMO-1–LUMO	1.54	1.50	1.51**	1.47
HOMO-1–LUMO +1	2.0	1.98	2.12**	2.02
HOMO-1–LUMO+2	1.86**	1.82	2.20**	2.22
HOMO-1–LUMO +3	1.91**	1.87	1.91**	1.87
HOMO-2–LUMO	3.43*	1.57	1.63**	1.55
HOMO-2–LUMO+1	2.09*	2.07	2.10**	2.08
HOMO-2–LUMO+2	1.94**	1.92	2.31**	2.31
HOMO-2–LUMO+3	1.99**	1.93	1.99**	1.93

Toluene is non-polar in nature. Using toluene as continuum, we have observed that the largest and the smallest values of CT excitations that are specified in bold faced letters as shown in the above table. The largest value of CT excitation energy is 3.43 eV in complex with ZnPc which corresponds to the transition HOMO-2–LUMO, which is favorable photo-energy production, and the smallest is 1.51 eV in two different transitions viz. HOMO–LUMO+1 and HOMO–LUMO+1. On the other hand, we have observed that there are more CT excitations with energy greater than 2 eV in the molecular complex with phthalocyanine in toluene. In contrast, there are no pure CT state in it. On the other hand, complex with ZnPc has four pure CT states which can be seen above. Thus, the molecular complex having Zn tends to serve as a better active material in OPVs.

3.3.5 Comparison of CT Excitation Energies

The calculated values of CT excitation energies for the molecular systems used for the study in three different dielectric and reported value of CT excitation energies in vacuum [12] are

compared. The plot below shows comparison of CT excitation energies (singlet) of Sc3N@C80–ZnPc for different transitions in water, acetone, toluene and reported gas values.

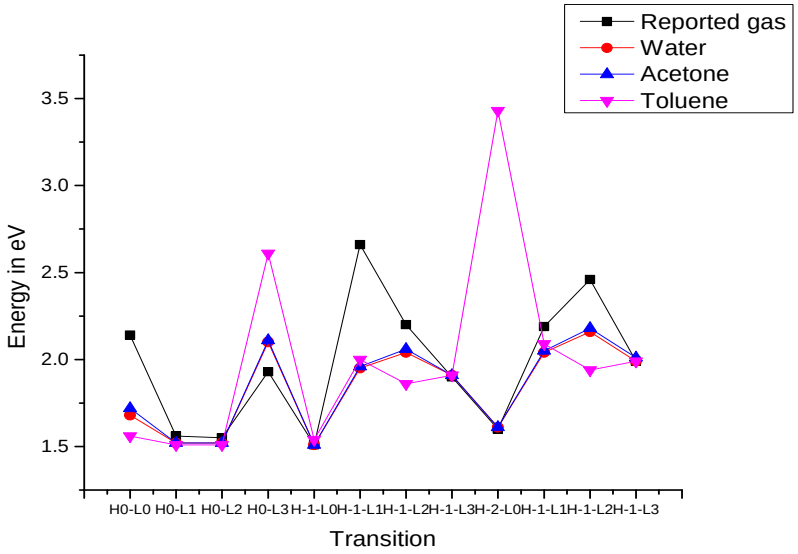

Figure 3.7: Plot of CT excitation energies (singlet state) of $Sc_3N@C_{80}$–ZnPc for different transitions in water, acetone, toluene and reported gas value.

In graph different transitions are labeled as H0-L0, H0-L1,.. respectively for transitions HOMO-LUMO, HOMO-LUMO+1 ... respectively. It is seen from the graph that the gas phase CT excitation energies of $Sc_3N@C_{80}$_ZnPc are more in the majority of the transitions than corresponding charge transfer excitation values of each solvents taken. On the one hand, toluene shows most charge transfer excitation energy in frontiers HOMO-LUMO+3 and HOMO-2-LUMO among water and acetone as well as in the gas phase. While for the other transitions, excitation energies lie at the bottom. Therefore in toluene, $Sc_3N@C_{80}$_ZnPc have some selective transition that are more favorable while others are less for POVs. In this complex, water and acetone show nearly same excitation energies for the corresponding charge transfer transitions while toluene goes on and off frequently. It may be due to the reason that reordering of excited state because of polarization.

Comparison of charge transfer excitation energies (singlet) of $Sc_3N@C_{80}$–H_2Pc for different transitions in water, acetone, toluene and reported value of gas as shown in the graph below.

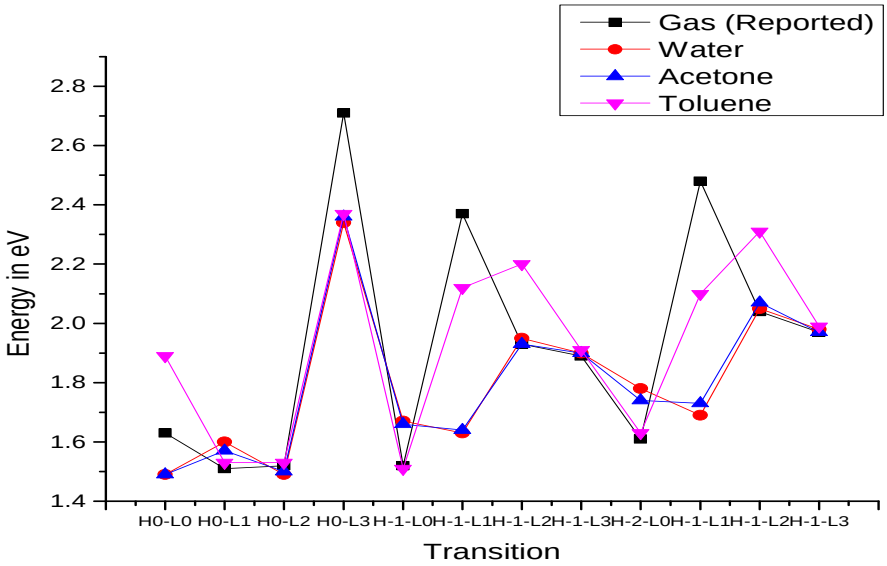

Figure 3.8: Comparison of charge transfer excitation energies (singlet) of $Sc_3N@C_{80}$–H_2Pc for different transitions in water, acetone, toluene and reported value of gas.

The trend of the charge transfer excitation energies of $Sc_3N@C_{80}$_H_2Pc for different transitions in the solvent taken and reported gas values charge transfer excitation energies for the corresponding transitions are seemed inconsistent. In some transitions, like HOMO-LUMO+3, HOMO-1-LUMO+1 and HOMO-2-LUMO+1, the reported value of charge transfer excitation energies in gas are more than observed values of energy in each of the solvent taken, which is as anticipated. While using toluene as solvent, this charge transfer complex possessed grater CT excitation energy to make electrons move form HOMOs to LUMOs.

Therefore non-polar solvent can be used to immerge chromophores for photo-voltaic application in order to achieve high photo-voltaic solar power generation The observed values of CT excitation energies in three different chosen solvents and the corresponding reported values of

CT excitations in gas showed that selection of solvent do not uniformly contribute for charge transfer while the polarity of solvent plays significant role.

3.4 DIPOLE MOMENTS IN EXCITED STATES

It is seen that dipole momenta of ground states for Sc_3NC_{80}–H_2Pc and Sc_3NC_{80}–ZnPc in gas phase are 1.4 D and 0.32 D. When these are studied in solutions, it is found that dipole moments of Sc_3NC_{80}–H_2Pc decrease on increasing the permittivity of the medium while gas phase ground state dipole moment is maximum in this complex. On the other hand, the dipole moment values of Sc_3NC_{80}–ZnPc in solution are increasing with the increasing polarity of the solution while the gas phase value remain at the bottom. The dipole moments of these complexes in different excited are obtained in solutions which are listed in tables below.

Table: 3.11: Dipole moments (in Debye) in excited state transition for the system in dielectric medium

Transitions (triplet state)	$Sc_3N@C_{80}$–ZnPc			$Sc_3N@C_{80}$_H_2Pc		
	Water	Acetone	Toluene	Water	Acetone	Toluene
HOMO–LUMO	27.5	27.56	26.21	5.6	5.71	4.39
HOMO–LUMO+1	1.15	1.22	1.43	17.66	16.6	6.97
HOMO–LUMO+2	0.4	0.33	0.28	7.71	7.06	3.14
HOMO-LUMO+3	27.67	26.9	27.9	30.36	30.25	29.72
HOMO-1–LUMO	1.85	1.7	0.64	16.95	17.77	4.17
HOMO-1–LUMO+1	21.74	20.44	14.68	14.56	15.30	21.05
HOMO-1–LUMO+2	28.36	27.49	21.21	27.86	26.31	14.37
HOMO-1–LUMO+3	2.81	2.63	0.63	2.24	2.16	0.96
HOMO-2- LUMO	1.55	1.43	0.58	16.64	15.47	3.86
HOMO-2–LUMO+1	21.8	20.46	15.07	14.49	15.25	21.31
HOMO-2–LUMO+2	28.86	28.04	21.42	28.5	26.88	14.23
HOMO-2–LUMO+3	2.63	2.44	0.31	1.36	1.27	0.66

Calculations have shown that for HOMO to LUMO transition (triplet) the dipole moments for Sc_3NC_{80}–ZnPc are 27.5 D, 27.56 D and 26.21D respectively in water, acetone and toluene. In contrast, these values for Sc_3NC_{80}–H_2Pc are 5.6 D, 5.71 D and 4.39 D respectively in water,

acetone and toluene. The reported value of gas phase dipole moments for Sc_3NC_{80}–ZnPc and Sc_3NC_{80}–H_2Pc for the HOMO to LUMO transition are 23.5 D and 8.7 D respectively. We can see that the transitions HOMO–LUMO, HOMO-LUMO+3, HOMO-1–LUMO +2, are HOMO-2–LUMO+2 are most likely to occur for the complex Sc_3NC_{80}–ZnPc in water and acetone, while for the toluene, the first two transitions occurs strongly and probability of occurrence of last two transitions mentioned occur relatively less among the most probable transitions. In case of Sc_3NC_{80}–H_2Pc, the transition HOMO–LUMO+3 occurs most strongly in each solvents while HOMO-1–LUMO+2, are HOMO-2–LUMO+2 occur fairly less frequently than HOMO–LUMO +3 in water and acetone and moderately in toluene. From the table of dipole moment, we can draw a conclusion that in most of the excited state dipole moment of the system of interest in dielectric decreases on decreasing the permittivity i.e. polarity.

Chapter 4: Conclusions

The ground state calculations of total energy of the electron-donor-acceptor molecular complexes in three different solutions have estimated correctly the total DFT energy for isolated molecular complexes with the error of few hundredth of electron volts. This established that the local PCM driver employed using UTEP NRLMOL codes is a correct solvation model to assess solvent effects. The errors are found to decreased if polarity decreases, which might indicate that electrostatic polarization provides less stabilization for the molecular complex in polar solvent than in non-polar solvents. Similarly, as expected, the electrostatic polarization energy is observed to be more for molecular complexes in non-polar solvent than in polar solvents because more energy is needed to polarize non-polar solvents than polar one. This is because that surface charges in the solute-solvent boundary spend work more to polarize the non-polar solvents. Further, the complex with zinc is found to have less electrostatic polarization energy than without zinc.

The calculations of vertical ionization potential of molecular system of interests in solvents showed that vIP is least for the systems in water and increases with increasing non-polarity of dielectric used for polarization. Among the three solvents used, vIP is most for toluene while least for water. Our calculations on each isolated solutes in DFT level showed even higher values of vIP. On the other hand, the calculated values of vertical electronic affinity for isolated molecular complex are reported less than our calculated values of vEA in dielectric medium. It is found that vEA of each complexes is most in water and least in toluene among the dielectric medium used. From these observations, we have concluded that when electron-donor-acceptor molecular complex placed in the dielectric of more polarity, it tends to lose electron easily (because of less vIP) and also tends to attract electrons difficulty (because of more vEA) in comparison to the systems in less polar or non-polar dielectric medium. Among the molecular system studied, $Sc_3N@C_{80}$–ZnPc is more favorable for electron-donor-acceptor pair in each dielectric medium studied than Sc3N@C_{80}–H_2Pc because Sc3N@C_{80}–H_2Pc has more vIP and vEA.

Wave functions analysis have disclosed that there are few pure CT states among the observed transitions in $Sc_3N@C_{80}$ – ZnPc while they are totally absent in $Sc_3N@C_{80}$ – H_2Pc for each of the dielectric medium used in this study. Among the isolated electron-donor-acceptor molecular pairs, $Sc_3N@C_{80}$ – ZnPc has some pure CT states. When the dielectric is toluene, the complex $Sc_3N@C_{80}$ – ZnPc exhibit four pure states for CT. Thus, $Sc_3N@C_{80}$ – ZnPc in toluene serves as a better active material in OPVs. Besides, pure CT, majority of transitions are partial CT states, which also enhance open circuit voltage of photovoltaic cells. The reverse CT might cause the recombination of charges so are not favorable OPVs.

The open circuit voltage is very sensitive and important factor in determining the power conversion efficiency of photovoltaic. The open circuit voltage is proportional to the charge transfer excitation energy. Among the dielectric taken for this study, $Sc_3N@C_{80}$ – H_2Pc in toluene possesses more CT excitation energies in majority of transitions while in water and acetone, it exhibits fewer more CT energies states than toluene. So, $Sc_3N@C_{80}$–H_2Pc in toluene is more favorable for photovoltaic application. On the other hand, the complex with ZnPc, the CT excitation energies in majority of transitions are found to be more or less equal. Being more pure charge transfer states for the system with ZnPc in toluene, it is expected to be a better option to increase the power OPVs if we use it as active materials.

While comparing the CT excitation energies of complexes studied in different polarizable medium, we have found that complex with ZnPc in water has more transitions that have slightly greater value of excitation energies than the excitation energies of complex without Zn for the corresponding transitions. This means that for water as polarizable medium, we can achieve better excitation energy and hence more open circuit voltage and efficiency for complex $Sc_3N@C_{80}$ – ZnPc as solute than complex with H_2Pc. If we use acetone as continuum medium, the same conclusions can be drawn as with water. In contrast, when toluene is used as continuum solvation medium, the CT excitation energies in the complex with H_2Pc have greater energy in majority

transitions than the complex with ZnPc. However, more pure charge transfer states are found in molecular complex with ZnPc, therefore again it is a preferred donor -acceptor complex for photovoltaic applications.

In summary, there are various factors that affect efficiency of OPVs. If we take open circuit voltage only into account, among $Sc_3N@C_{80}$–ZnPc and $Sc_3N@C_{80}$–H_2Pc, complex with ZnPc can perform better than complex with H_2Pc as active layer. Further, due to reordering and polarization effect, there is more stabilization in non-polar dielectric than polar dielectric continuum medium. Therefore, greater excitation energy are expected in the non-polar solvents which might help in achieving greater power conversion from the incident electromagnetic radiations on active layer of photovoltaic.

Reference

[1] D. Wöhrle and D. Meissner, Advanced Materials **3**, 129 (1991).

[2] C. J. Brabec and V. Dyakonov, in *Organic Photovoltaics: Concepts and Realization*, edited by C. J. Brabec, V. Dyakonov, J. Parisi, and N. S. Sariciftci (Springer Berlin Heidelberg, Berlin, Heidelberg, 2003), pp. 1–56.

[3] H. Hoppe and N. S. Sariciftci, Journal of Materials Research **19**, 1924 (2004).

[4] T. H. Le, Y. Kim, and H. Yoon, Polymers **9**, (2017).

[5] L. M. Popescu, *Fullerene Based Organic Solar Cells Popescu, Lacramioara Mihaela* (2008).

[6] T. L. Benanti and D. Venkataraman, Photosynthesis Research **87**, 73 (2006).

[7] C. J. Brabec, A. Cravino, D. Meissner, N. S. Sariciftci, T. Fromherz, M. T. Rispens, L. Sanchez, and J. C. Hummelen, Advanced Functional Materials **11**, 374 (2001).

[8] S. Günes, H. Neugebauer, and N. S. Sariciftci, Chemical Reviews **107**, 1324 (2007).

[9] M. Olguin, L. Basurto, R. R. Zope, and T. Baruah, The Journal of Chemical Physics **140**, 204309 (2014).

[10] D. Gust, T. A. Moore, and A. L. Moore, ChemInform **41**, (2010).

[11] L. Basurto, F. Amerikheirabadi, R. Zope, and T. Baruah, Physical Chemistry Chemical Physics **17**, 5832 (2015).

[12] F. Amerikheirabadi, C. Diaz, N. Mohan, R. R. Zope, and T. Baruah, Physical Chemistry Chemical Physics **20**, 25841 (2018).

[13] C. M. Cardona, A. Kitaygorodskiy, and L. Echegoyen, Journal of the American Chemical Society **127**, 10448 (2005).

[14] L. Echegoyen and L. E. Echegoyen, Accounts of Chemical Research **31**, 593 (1998).

[15] J. M. Campanera, C. Bo, M. M. Olmstead, A. L. Balch, and J. M. Poblet, The Journal of Physical Chemistry A **106**, 12356 (2002).

[16] M. Linares, D. Beljonne, J. Cornil, K. Lancaster, J.-L. Brédas, S. Verlaak, A. Mityashin, P. Heremans, A. Fuchs, C. Lennartz, J. Idé, R. Méreau, P. Aurel, L. Ducasse, and F. Castet, The Journal of Physical Chemistry C **114**, 3215 (2010).

[17] M. R. Cerón, M. Izquierdo, N. Alegret, J. A. Valdez, A. Rodríguez-Fortea, M. M. Olmstead, A. L. Balch, J. M. Poblet, and L. Echegoyen, Chemical Communications **52**, 64 (2016).

[18] M. N. Chaur, F. Melin, A. J. Athans, B. Elliott, K. Walker, B. C. Holloway, and L. Echegoyen, Chemical Communications 2665 (2008).

[19] R. R. Zope, M. Olguin, and T. Baruah, Journal of Chemical Physics **137**, (2012).

[20] T. Baruah, M. Olguin, and R. R. Zope, Journal of Chemical Physics **137**, (2012).

[21] X. Lu, L. Feng, T. Akasaka, and S. Nagase, Chemical Society Reviews **41**, 7723 (2012).

[22] T. Baruah and M. R. Pederson, Journal of Chemical Theory and Computation **5**, 834—843 (2009).

[23] R. S. Mulliken, Journal of Physical Chemistry **56**, 801 (1952).

[24] B. P. Rand, D. P. Burk, and S. R. Forrest, Physical Review B - Condensed Matter and Materials Physics **75**, 1 (2007).

[25] T. Ziegler, A. Rank, and E. J. Baerends, Acta (Berl.) **43**, 261 (1977).

[26] R. M. Martin, Cambridge University Press (2004).

[27] S. Demers, **2014**, 160 (2014).

[28] B. T. Sutcli and R. G. Woolley, (2012).

[29] I. Gilbert, **1**, (1975).
[30] C. Physics, (n.d.).
[31] J. P. Perdew, K. Burke, and M. Ernzerhof, Phys. Rev. Lett. **78**, 1396 (1997).
[32] J. Tomasi, B. Mennucci, and R. Cammi, Chemical Reviews **105**, 2999 (2005).
[33] B. Mennucci, Wiley Interdisciplinary Reviews: Computational Molecular Science **2**, 386 (2012).
[34] G. Scalmani, M. J. Frisch, B. Mennucci, J. Tomasi, R. Cammi, and V. Barone, Journal of Chemical Physics **124**, (2006).
[35] J. L. Pascual-ahuir, E. Silla, and I. Tuñon, Journal of Computational Chemistry **15**, 1127 (1994).
[36] P. CS, T. J, and C. R., Journal of Computational Chemistry **22**, 1262 (2001).
[37] L. Frediani, R. Cammi, C. S. Pomelli, J. Tomasi, and K. Ruud, Journal of Computational Chemistry **25**, 375 (2004).
[38] M. Mantina, A. C. Chamberlin, R. Valero, C. J. Cramer, and D. G. Truhlar, The Journal of Physical Chemistry A **113**, 5806 (2009).
[39] E. Cancès, B. Mennucci, and J. Tomasi, The Journal of Chemical Physics **107**, 3032 (1997).
[40] B. Mennucci, E. Cancès, and J. Tomasi, The Journal of Physical Chemistry B **101**, 10506 (1997).
[41] S. Miertus, E. Scrocco, and J. Tomasi, Chemical Physics **55**, 117 (1981).
[42] A. Klamt and G. Schuurmann, J. Chem. Soc. Perkin Trans 2 799 (1993).
[43] V. Barone and M. Cossi, The Journal of Physical Chemistry A **102**, 1995 (1998).
[44] H. Li and J. H. Jensen, Journal of Computational Chemistry **25**, 1449 (2004).
[45] (n.d.).
[46] M. R. Pederson and K. A. Jackson, Phys. Rev. B **43**, 7312 (1991).
[47] K. Jackson and M. R. Pederson, Phys. Rev. B **42**, 3276 (1990).
[48] M. R. Pederson and K. A. Jackson, **41**, 7453 (1990).
[49] A. A. Quong, M. R. Pederson, and J. L. Feldman, Solid State Communications **87**, 535 (1993).
[50] Q. Wu and T. Van Voorhis, Physical Review A - Atomic, Molecular, and Optical Physics **72**, 7 (2005).
[51] F. Amerikheirabadi, R. R. Zope, C. Tunna Baruah, C. W. Dirk, and C. Ambler, *ELECTRONIC STRUCTURE AND CHARGE TRANSFER EXCITED STATES OF ENDOHEDRAL FULLERENE CONTAINING ELECTRON DONOR-ACCEPTOR COMPLEXES UTILIZED IN ORGANIC PHOTOVOLTAICS* (n.d.).
[52] M. Olguin, R. R. Zope, and T. Baruah, Journal of Chemical Physics **138**, (2013).

Vita

Surya Prasad Timilsina was born in Pokhara, Nepal. He is the youngest son of the Durga Datta Timilsina and Lali Timilsina. He graduated from the high school in 2006. After that he started Bachelor Degree in Physics in 2006 at Prithvi Narayan Campus and then in 2010 he started his Master degree in physics from the same campus. He received his master's degree in physics in 2014 with first division. He joined the University of Texas at El Paso as a graduate student in 2017 and graduated MS physics in 2019, where he got a chance to work as TA.

Email: sptimilsina@miners.utep.edu or sisforaim@gmail.com

The author typed this thesis.